Optimization of the production of lipids and carotenoids in the microalga *Golenkinia* aff. *brevispicula*

Rearte, T.A.[1,2*]; Figueroa, F.L. [3]; Gómez-Serrano C. [4]; Vélez, C.G.[5]; Marsili S.[1,5]; Iorio A. de F.[1]; González-López, C.V. [4], Cerón-García, M.C.[4]; Abdala, R.[3]; Acién, F.G.[4]

1 Departamento de Recursos Naturales y Ambiente, Facultad de Agronomía, Universidad de Buenos Aires, CABA, Av. San Martín 4453, 1417 Buenos Aires, Argentina

2 Consejo Nacional de Investigaciones Científicas y Técnicas (CONICET), Argentina

3 Universidad de Málaga. Instituto de Biotecnología y Desarrollo Azul (IBYDA) Departamento de Ecología, Facultad de Ciencias, Campus Universitario de Teatinos s/n, 29071 Málaga, Spain

4 Department of Chemical Engineering, Universidad de Almería, E04120 Almería, Spain

5 Departamento de Biodiversidad y Biología Experimental, Facultad de Ciencias Exactas y Naturales, Instituto de Micología y Botánica, UBA-CONICET, CABA, Piso 4, Pabellón II, Lab 68, Av. Int. Güiraldes 2620, C1428EHA Buenos Aires, Argentina.

***corresponding author: tarearte@agro.uba.ar**

Abstract

Microalgae are a promising platform to produce natural pigments and lipids when compared to traditional sources, since they present faster growth and biomass

productivity and there is a wide diversity that has not been studied yet. The green microalgae belonging to the genus *Golenkinia* presents few reports of its biomass production and applications. In this work, the productivity of lipids and carotenoids was studied in the strain *Golenkinia* aff. *brevispicula* FAUBA-3 using a two-stage cultivation system: a first step for biomass production under semicontinuous cultures, and a second step for the accumulation of lipids and carotenoids under batch salinity stress (35 g L^{-1}). The highest biomass productivity (0.92 g L^{-1} d^{-1}) was obtained under a dilution rate of 0.4 d^{-1}. The growth rate (μ) was a hyperbolic function of average irradiance inside the culture (E_{av}). The optimum E_{av} was 88.4 µmol photons m^{-2} s^{-1} and the maximum specific growth rate (μ_{max}) was 0.85 d^{-1}. Photoinhibition was observed above 570 µmol photons m^{-2} s^{-1} of E_{av}. The best photosynthetic performance was obtained at 0.2 d^{-1} dilution rate but with lower biomass productivity due to nutrients and light limitation. High content of protein (30 % DW) and polyunsaturated fatty acids (50% of total PUFAs) and low content of carbohydrates (19 % DW) were observed at high dilution rate, and the opposite response at low dilution rate. In the second culture stage, an increase of salinity induced lipid and carotenoid accumulation which improved the productivity to 89 mg L^{-1} d^{-1} and 1.3 mg L^{-1} d^{-1} of total lipids and carotenoids respectively compared to one-stage culture. Lutein, β-carotene and astaxanthin were the main carotenoid identified in a decreasing order. Those results confirm that two-stage culture is an adequate strategy to optimize the carotenoid and lipid productivity in the promising strain *Golenkinia* FAUBA-3.

Key words: *Golenkinia*; Two-stage Culture; Lipid; Carotenoid; Productivity

1. Introduction

The role of polyunsaturated fatty acids (PUFAs) and carotenoids in human health and animal feed has acquired relevance in recent years, mainly for their nutraceutical, cosmetic and pharmaceutical properties with emphasis in compounds obtained from natural sources [1–3]. This demand has promoted large-scale cultivation of microalgae for the production of high-value compounds like carotenoid and PUFAs [4]. The well-accepted effect of carotenoids, especially astaxanthin and β-carotene [5], to prevent and treat degenerative diseases has indeed opened new avenues. Another important carotenoid is lutein, which has gained increasing attention as the result of recent studies. It has been demonstrated that an adequate intake might help to prevent, or ameliorate, the effects of degenerative eye diseases such as age-related macular degeneration [6,7] through attenuation apoptosis and autophagy in glial cell [8]; and in skin health [9]. Currently, lutein is obtained from marigold petals. However, it presents several drawbacks as a lutein source given the low lutein content in the petals [10].

Advances in knowledge of physiology, molecular pathways, and biochemistry have helped to understand the mechanism of carotenoids and lipids accumulation in microalgae, which would allow to control and manipulate culture conditions in order to enhance the productivity of compounds of interest. Several studies showed that under abiotic stress (*e.g.* light intensity, UV radiation, salinity, temperature, and nutrient limitation) microalgae undergo strong metabolic changes in their physiology and biochemistry producing significant amounts of secondary metabolites (*i.e.* carotenoids and lipids reserves) as a protection mechanism [11–16]. However,

under these limiting conditions the growth is strongly affected, and the biomass productivity is reduced. According to Griffiths and Harrison [17], the biomass productivity is the most relevant factor that determine the lipid productivity in any microalgal species. To overcome the challenges of biomass productivity and stress induction, two-stage cultivation systems is recommended, since in a first step microalgae are grown under optimal conditions to maximize biomass production, and in a second step the cultivation conditions are modified to trigger the accumulation of carotenoids and lipids [12,16].

Currently, the global market of carotenoids from algae is mainly comprised of astaxanthin from *Haematococcus pluvialis* and β-carotene from *Dunaliella salina* produced by various companies around the world [4]. Both species presents the advantage of accumulating high carotenoid content but under low biomass productivity. Therefore, it is necessary to explore new robust species with high biomass productivity to produce carotenoids including others than astaxanthin and β-carotene. Scarce studies focused on growth and metabolite accumulation have been conducted in the green microalgae *Golenkinia*. Recently, Rearte et al. [15] described the cellular stages and the accumulation of carotenoid and lipids in a promising strain of *Golenkinia* aff. *brevispicula* FAUBA-3 induced by increased salinity, but with a low biomass productivity under batch culture (0.1 g L^{-1} d^{-1}). An alternative strategy to obtain higher biomass productivity than under batch operation, is semi-continuous cultures, which has the advantage of controlling light and nutrients availability by manipulation of dilution rate. High dilution rate provides high nutrients availability, and a low biomass concentration which also implies less self-shading (*i.e.* higher light availability) than low dilution rates. It is already known that

nutrients and light availability modify the physiological and biochemical state of microalgae [16]. Therefore, the different dilution rates could be used to control the physiological state of cells before the stress phase, an important factor that determines the extension and rate of the accumulation of secondary metabolites.

The aim of this work was to optimize the production of lipids and carotenoids of the strain *Golenkinia* aff. *brevispicula* FAUBA-3 (further as *Golenkinia* FAUBA-3) using a two-stage culture strategy. In a first culture stage, optimization of the dilution rate under semi-continuous operation mode was performed for enhancing biomass productivity. In a second culture stage, a batch stress was applied by increasing of salinity to induce lipids and carotenoids accumulation. We have used several physiological approaches including growth model, biochemical parameters, and photosynthetic performance by *in vivo* chlorophyll *a* fluorescence measurement to elucidate the effect of the different culture stages on the productivity and physiology of the strain *Golenkinia* FAUBA-3.

2. Material and Methods

2.1. Microalgae and culture conditions

Golenkinia aff *brevispicula* FAUBA-3 was isolated from a freshwater pond located in the campus of Facultad de Veterinaria (Universidad de Buenos Aires), Buenos Aires, Argentina (34°35'40.8"S; 58°28'52.6"O) at May 2012 as described previously [15]. Cultures were grown and maintained in liquid Jaworski´s freshwater Medium (JM) in 250 mL Erlenmeyer flasks containing 80 mL of culture, at 40 µmol photons m^{-2} s^{-1} PAR 12:12 (L:D) photoperiod and 23-25ºC deposited in the *ad hoc* culture collection of our laboratory (Facultad de Agronomía, Universidad de Buenos Aires,

Argentina). Pre-inocula were cultured in 1 L bubbled column-type reactors for 9 days with 800 mL of Arnon media [18] at a continuous irradiance of 300 µmol photons m^{-2} s^{-1} PAR at 25 ± 1ºC in a controlled chamber. Continuous bubbling of atmospheric air filtered through 0.22 µm sterile filters was performed and CO_2 was injected on demand (pH > 8) in the air flow entering the reactor.

2.2. Two-stage cultures: semi-continuous biomass production and batch stress phase

Experiments were performed in 12 bubbled column-type photobioreactors with spherical bases (3 cm inner diameter and 45 cm height with 300 mL capacity) filled with 250 mL of media. The reactors were continuously aerated with filtered (0.22 µm) atmospheric air at a rate of 0.2 vvm and CO_2 was injected into the air flow entering the cultures to maintain pH=8 controlled by a pH sensor (Crison Instruments®) during the growth phase. The culture temperature was monitored and kept at 25±2°C by controlling the room temperature where the reactors were located. The photobioreactors were irradiated by artificial illumination using eight fluorescent white-light tubes of 28 W (Philips Daylight T5) positioned horizontally to the reactors. Incident irradiance was applied simulating solar cycle with a photoperiod of 12:12 with increasing light intensity at midday and decreasing after midday (8 to 9:30 h: 317 µmol photons m^{-2} s^{-1}; 9:30 to 11 h: 662 µmol photons m^{-2} s^{-1}; 11 to 12:30 h: 866 µmol photons m^{-2} s^{-1}; 12:30 a 15:30 h: 982 µmol photons m^{-2} s^{-1}; 15:30 to 17 h: 866 µmol photons m^{-2} s^{-1}; 17 to 18:30 h: 662 µmol photons m^{-2} s^{-1}; 18:30 to 20 h: 317 µmol photons m^{-2} s^{-1}). The irradiance was measured at the inner surface of reactors using a spherical quantum sensor SQS-100 Walz GmbH (Effeltrich, Germany). All

the experiments were carried out in triplicate. Inoculum was performed in batch mode until reach stationary phase of growth using medium Arnon.

Two-stage cultures were performed: in a first step semi-continuous cultures were applied for the growth phase, and in a second step a salinity stress in batch mode was applied to induce lipid and carotenoid accumulation. Semi-continuous cultures were operated at four dilution rates (D): 0.2, 0.4, 0.6, and 0.8 d^{-1}. Each volume culture was renewed every 24 h during the first hours of the light period with fresh medium throughout ten days to ensure two complete renewals of total reactor volume in each dilution rate. Salinity stress was applied at day ten by adding marine salt (Flor de Sal Cabo de Gata, Almeria, Spain) to the culture in a concentration of 35 g L^{-1} and they were operated in batch regime for six days.

2.3. Growth measurements and optical properties

Growth was monitored by optical density and cell dry weight (DW). DW (g L^{-1}) was measured by filtering 10 mL aliquot of the culture through pre-weighed dry filters (Whatman GF/C 47 mm and 1.2 µm glass fiber filters). The filters were washed with 10 mL of distilled water, dried in an oven at 70 ºC and reweighed until a constant weight was achieved. Optical density was measured in a double beam Helios Alpha spectrophotometer at 680 nm and it was correlated to cell dry weight (DW = 0.9096 x abs_{680nm}; r^2 = 0.97). The biomass extinction coefficient (Ka) was calculated from absorption value of the suspension in the visible range (abs 400-700 nm, light source: 150 W halogen lamp) measured by a cosine corrected PAR sensor (Licor192SA 400-700 nm) connected to a radiometer (Li-250A) both from Licor (USA) according to Jerez et al. [19]. The Ka (m^2 g DW^{-1}) was estimated based on the following equation (Eq. 1):

$$\mathrm{Ka} = \frac{-\ln\left(\frac{E}{E_0}\right)}{\mathrm{DW} \cdot p} \quad (1)$$

where E_o is the transmitted irradiance of the fresh medium and E is the transmitted irradiance of the culture suspension, p is the cuvette light path (0.003 m) and DW is dry weight (g m^{-3}). *In vivo* chlorophyll *a*-specific absorption cross-sections of the suspension [a^*, (m^2 mg^{-1} Chl *a*)] was estimated on the following equation (Eq. 2):

$$a^* = \frac{-\ln\left(\frac{E}{E_0}\right)}{[Chl\ a] \cdot p} \quad (2)$$

where [Chl *a*] is chlorophyll *a* concentration expressed in mg m^{-3}. The average irradiance inside the culture (E_{av}; µmol photons m^{-2} s^{-1}) was calculated as a function of the surface irradiance (E_o; µmol photons m^{-2} s^{-1}), the biomass extinction coefficient (Ka), the biomass concentration (g DW m^{-3}) and the light path inside the reactor (p, m) (Eq. 3).

$$E_{av} = \frac{E_0}{\mathrm{Ka\ DW}\ p}\left(1 - e^{(-\mathrm{Ka\ DW}\ p}\right) \quad (3)$$

At steady-state condition (µ = D) the specific growth rate (µ; d^{-1}) was fitted to a hyperbolic function to describe the relationship between the growth rate and average irradiance [20] (Eq. 4)

$$\mu = \mu_{max} \frac{E_{av}^n}{E_k^n + E_{av}^n} \quad (4)$$

where μ_{max}, E_k, and n are the maximum specific growth rate (d^{-1}), the average irradiance affinity constant (µmol photons m^{-2} s^{-1}), and a characteristic shape

parameter respectively. The data of the last three days under steady state condition (n = 36) were used for fitting the model and parameter estimation.

2.4. *In vivo* chlorophyll *a* fluorescence measurement

*In viv*o chlorophyll *a* fluorescence associated to photosystem II was determined by Pulse Amplitude Modulated (PAM) fluorimeters. F_o (basal fluorescence from fully oxidized reaction centres of PSII) and F_m (maximal fluorescence from fully reduced PSII reaction centres), were determined in darkness to obtain the Maximal Quantum Yield (Fv/Fm) being Fv the difference between Fm and Fo [21]. The Fv/Fm was measured daily (AquaPenAP 100, Photon Systems Instruments, Drasov, Te Czech Republic) to monitor the physiological status of cells. Rapid Light Curves (RLCs) by using blue light as measuring, actinic and saturating pulse lights (Junior PAM, Walz GmbH, Effeltrich, Germany) were performed according to Schreiber et al. [21]. Dark-adapted samples (15 min) were exposed to twelve increasing actinic irradiances (25-45-66-90-125-190-285-420-625-845-1150-1500 µmol photons m^2 s^{-1}) for 20 s at each one in a light-protected measuring chamber (15 mL). Light-adapted fluorescence level F' and the maximum fluorescence level F_m' at the end of each step of saturating pulse were recorded. The actual PSII photochemical quantum yield in the light, Y(II) or $\Delta F/F_m'$, was determined as $(F_m' - F')/F_m'$ at respective irradiance level. The electron transport rate (ETR) through PSII per chlorophyll *a* unit (µmol e^- mg Chl a^{-1} s^{-1}) was determined as follows:

$$\mathrm{ETR}^* = \Delta \mathrm{F}/\mathrm{Fm}' \times \mathrm{E}_{\mathrm{PAR}} \times a^* \times f\mathrm{QA}_{\mathrm{PSII}} \quad (5)$$

where E_{PAR} is the incident photosynthetically active irradiance (µmol photons m^{-2} s^{-1}), *a** is the chlorophyll-specific absorption cross-sections [*a**, (m^2 mg^{-1} Chl *a*)] and

*f*AQA$_{PSII}$ is the fraction of absorbed quanta by PSII, 0.51 for Chlorophyceae (taken from [22]). The ETR per biomass unit (µmol e^- g DW^{-1} s^{-1}) was determined as follows:

$$\mathrm{ETR}_B = \Delta \mathrm{F/Fm'} \times \mathrm{E_{PAR}} \times \mathrm{Ka} \times f\mathrm{QA_{PSII}} \quad (6)$$

where Ka is the biomass extinction coefficient (m^2 g DW^{-1}). ETR was plotted vs irradiance to obtain the P-E curves. The curves were fitted by non-linear least-squares regression using the tangential function reported by Eilers and Peeters [23] to estimate P-E curve parameters: maximum ETR (ETR_{max}), the initial slope of ETR vs. E_{PAR} (alpha, α) as an estimator of photosynthetic efficiency, onset of irradiance saturating photosynthesis ($E_{k\ PSII}$) and irradiance of the initial photoinhibition ($E_{opt\ PSII}$). Non-photochemical quenching [NPQ = (Fm-Fm´)/Fm´] of the fluorescence is a measure of energy dissipation and as the ratio of yield losses Y(NPQ)/Y(NO), being Y(NPQ) a photoregulated yield loss through xanthophyll cycle and Y(NO) non photoregulated thermal dissipation. Y(NPQ) and Y(NO) are inversely related to photochemistry (Y(II)) and NPQ is considered an indicator of photoprotection to the excess of irradiance [24]. NPQmax was obtained from the tangential function of NPQ versus irradiance according to [23].

Definitions and abbreviations used are reported in Table 1.

2.5. Biochemical Analysis

Centrifuged biomass was washed twice with distilled water, freeze-dried and stored in dark conditions at -20 ºC until biochemical analysis. For all analyses, cellular disruption was performed by biomass milling in a mortar and then agitating it in glass tubes with glass beads (diameter 2 mm) and the specific solvent on vortex in the dark. Total lipids were extracted with chloroform:methanol (2:1) (*v/v*) and

purified according to Folch et al. [25] adapted to microalgal samples. Extracted lipids were quantified by the gravimetric method. Total soluble carbohydrates were extracted with 0.1 N HCl at 95 ºC in a water bath for 1 h (pigments were removed from the biomass previously with ethanol). Carbohydrates were measured in the extract following the methods of McCready et al. [26] modified by Brányiková et al. [27] using perchloric acid (30%) to hydrolyze starch. The soluble carbohydrate extract was mixed with anthrone solution (2g anthrone in 1L of 72 % H_2SO_4), heated in a water bath at 100ºC for 8 min, and the absorbance was measured at 625 nm after cooling the samples at room temperature. Calibration was carried out simultaneously using glucose as the standard (24 – 12 mg L^{-1}). The total internal nitrogen was determined by using a CNHS LECO -932 elemental analyzer (MI, USA) and proteins was estimated using the N-Prot conversion factor of 4.78 according to Lourenço et al. [28]. Pigments were extracted with DMSO for 16 h at 4 °C in the dark. The extraction procedure was repeated until the cells became visibly colorless. The different pigments (Chl a; Chl b; Total carotenoids) were calculated according to Wellburn [29].

For the analysis of fatty acid profiles the lipids were trans-esterified according to the method described by Christie (1982). The dried residue after lipid determination was resuspended with toluene with butylated hydroxytoluene (BHT) 50 mg L^{-1} and methylated with 2 mL of H_2SO_4:CH_3OH 1% v/v solution at 50 °C for 16h in the dark under N_2 atmosphere. The fatty acid methyl esters (FAMEs) were extracted twice with 4 mL of hexane:diethyl ether 1:1 with BHT 0.01% and washed three times with 3 ml of $KHCO_3$ 2%. The hexane phase was separated by centrifugation, filtered through a Sep-Pak Aminopropyl (NH2) cartridges (Waters, Mildford, Massachusetts,

USA) and evaporated to dryness under a stream of N_2 (g). Chromatographic-grade hexane was added to a final volume of 50 µL. FAMEs were separated by gas chromatography (Focus GC, Thermo Scientifics) using He as a carrier gas with a forte BPX70 (70% cyanopropyl polysilphenylene-siloxane) 60 m x 0.25 mm column (SGE analytical science). The initial temperature of the column was set to 140 ºC for 10 min, then it was raised to 240ºC at 2.5 ºC min^{-1} and finally maintained at 240º C for another10 min period. Detection was performed by a flame ionization detector and the peaks were identified with a FAME standard mix (Supelco 37 Component FAME Mix, Sigma-Aldrich Corp).

Individual carotenoids were analyzed by high performance liquid chromatography (Shimadzu SPDM10AV HPLC) using a photodiode array detector as described by Cerón-García et al. [31]. Samples (5 mg) were disrupted with alumina in a mortar and extracted in glass Pyrex tubes with 1 mL of monophasic tricomponent solution (ethanol:hexane:water, 77:17:6 v/v/v) until the extract was clear. The water fraction contained 20 % d.w. potassium hydroxide (g KOH g DW^{-1}) for carotenoid saponification. The tubes were vortexed for 2 min and subsequently, they were centrifuged at 12000 rpm for 2 min (Mini Spin Plus, Eppendorf) and the supernatant was transferred into a vial ready to be analysed by HPLC. The HPLC procedure was as described by Cerón-García et al. [32]. Separation was performed on a Lichrosphere RP-18 5 µm column (4.6 x 150 mm). The eluents used were (A) water/methanol (2:8, v/v) and (B) acetone/methanol (1:1 v/v). The pigments were eluted at a rate of 1 mL min^{-1} and detected by measuring absorbance at 360-700 nm. Standards of lutein, astaxanthin and β-carotene were provided by Sigma

Chemical Co. (USA) while violaxanthin and zeaxanthin standards were purchased from DHI Lab Products (Hørsholm, Denmark).

2.6. Statistical analyses

Descriptive statistics (average and standard deviation) were used to present the data. Statistical differences between treatments were tested by one-way ANOVA using the software R. A posteriori comparison was made using Tukey's test (α = 0.05). When the data did not adjust to a normal distribution and homogeneity of variance assumptions, statistical differences were tested by one-way ANOVA permutation test using the software R. A generalized lineal model (GLM) using an unstructured covariance matrix was used to analyze differences of biomass concentration in function of culture time according to a repeated measures experiment. Nonlinear regression was performed using the software Statgraphics 18.

Table 1. Symbols and abbreviations descriptions.

Symbols	Units	Description
Ka	m^2 g DW^{-1}	Biomass extinction coefficient
a*	m^2 mg Chl^{-1}	*In vivo* chlorophyll *a*-specific absorption cross-sections of the suspension
E_{PAR}	µmol photons m^{-2} s^{-1}	Photosynthetically active irradiance
E*av*	µmol photons m^{-2} s^{-1}	Average irradiance inside the culture
µ	d^{-1}	Specific growth rate

μ_{max}	d^{-1}	Maximum specific growth rate
E_k	µmol photons m^{-2} s^{-1}	Average irradiance affinity constant of growth rate
Chl *a*		Chlorophyll a
Fv/Fm		Maximum quantum yield of PSII
RLC		Rapid Light Curve
ETR*	µmol e^- mg Chl^{-1} s^{-1}	Electron transport rate per Chl *a* unit
ETR_B	µmol e^- g DW^{-1} s^{-1}	Electron transport rate per biomass unit
α		Initial slope of ETR vs E_{PAR}
NPQ		Non photochemical quenching
$E_{k\ PSII}$	µmol photons m^{-2} s^{-1}	Onset of irradiance saturating photosynthesis
$E_{opt\ PSII}$	µmol photons m^{-2} s^{-1}	Irradiance of the initial photoinhibition

3. Results and discussion

3.1. Biomass production and photosynthetic performance

In the first culture stage, different dilution rates under semicontinuous mode were evaluated to optimize the biomass productivity of *Golenkinia* FAUBA-3. Figure 1A shows the biomass concentration as a function of the culture time for all dilution rates. Steady-state was reached around day 6 in all treatments except for the dilution rate of 0.8 d^{-1} in which a washout of the biomass was observed and this treatment was not further analysed (Figure 1A). Therefore, the maximum dilution rate that can

be operated for this strain should be less than 0.8 d^{-1}. This is in concordance with Rearte et al. [15] who reported a maximum specific growth rate of 0.78 d^{-1} in a batch culture of *Golenkinia* FAUBA-3.

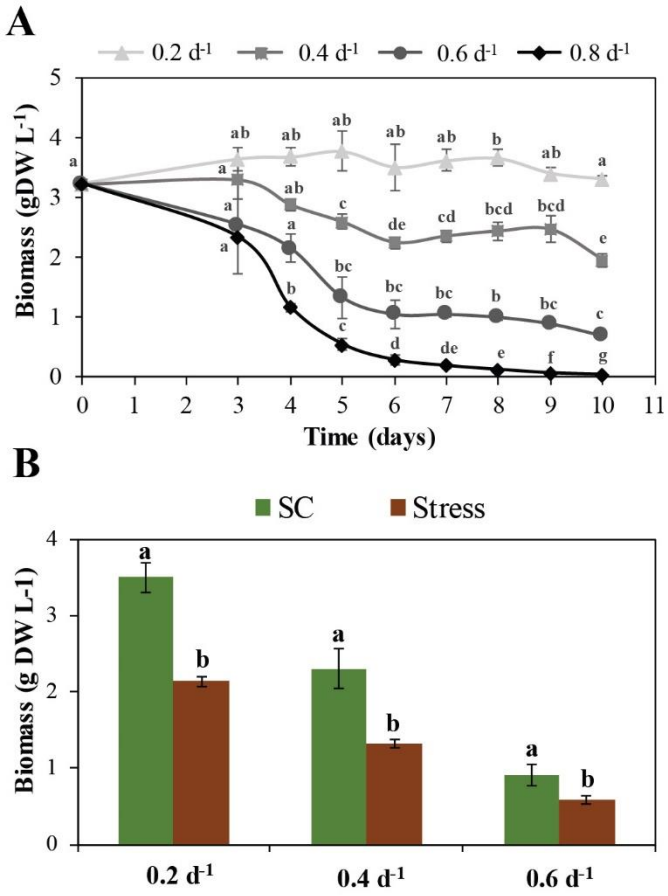

Figure 1. Biomass concentration of *Golenkinia* FAUBA-3 under a two-stage culture system. **(A)** Time course of biomass concentration under semicontinuous cultures (SC) at 0.2, 0.4, 0.6 and 0.8 d^{-1} dilution rates. Different letters indicate significant differences of means between the different days in one treatment ($p<0.05$). **(B)** Biomass concentration at steady-state condition under semicontinuous cultures (average data from day 7 to day 10) and at final day of batch salinity stress. Data are the means and standard deviation of three replicate experiments. Different letters indicate significant differences of means between SC and stress cultures ($p<0.05$).

Steady-state biomass concentration decreased with dilution rates: 3.5, 2.3, and 0.91 g DW L^{-1} were observed at 0.2, 0.4, and 0.6 d^{-1} dilution rates respectively (Figure 1B). A similar tendency in other microalgal species was observed by Bermúdez et al. [33] and Jebali et al. [34] according to a typical trend where the biomass concentration decreased as the dilution rate increased. In the second culture stage, biomass concentration showed a slightly decrease under salinity stress in batch mode (Figure 1B) which would indicate a loss of biomass by cell death. Figure 2 shows the different cell colours observed under microscopy. Figure 2A-B shows different orange and green-orange cells with bristles under salinity stress according to the presence of carotenoid. Figure 2C shows bleached cells (probably death cells). The highest biomass productivity (0.92 g L^{-1} d^{-1}) was obtained at 0.4d^{-1} dilution rate (Table 2) which is far higher than that obtained in a culture of *Golenkinia* FAUBA-3 under batch mode (0.1 g L^{-1} d^{-1}) [15].

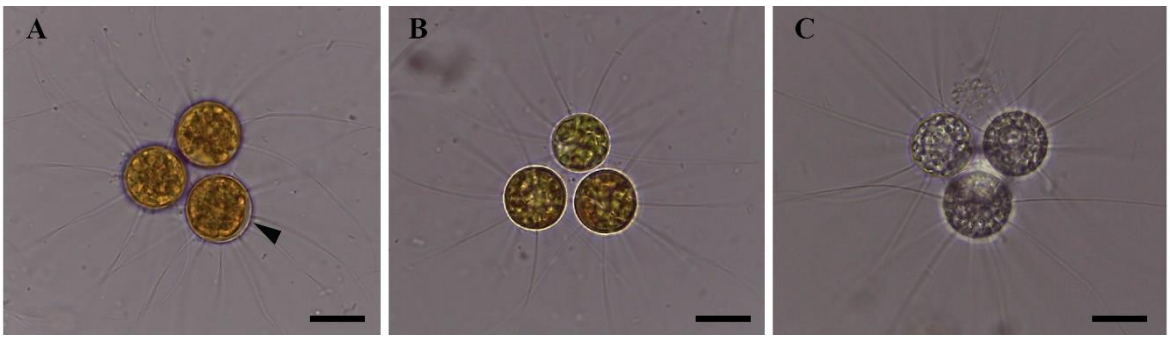

Figure 2. Light microscopy images of various cells of *Golenkinia* FAUBA-3 under salinity stress. **(A)** Completely reddish-orange cells (D = 0.4 d^{-1}) with the cell wall with bristles showing slightly plasmolysis (arrow). **(B)** Presence of reddish-orange-green cells (D = 0.2 d^{-1}). **(C)** Bleached non-viable cells (D = 0.6 d^{-1}). Scale bar 10 μm.

Table 2. Volumetric productivity of biomass, lipid and carotenoid of *Golenkinia* FAUBA-3 under semicontinuous cultures at steady-state condition under different dilution rates and salinity stress. Data are the means and standard deviation of three replicate experiments. Different letters indicate significant differences of means ($p<0.05$).

	Semicontinuous cultures		
	Biomass (g L^{-1} d^{-1})	**Lipids (mg L^{-1} d^{-1})**	**Carotenoids (mg L^{-1} d^{-1})**
0.2d^{-1}	0.70 ± 0.00 a	37.4 ± 2.1 a	0.15 ± 0.03 a
0.4d^{-1}	0.92 ± 0.06 b	73.5 ± 7.2 b	0.69 ± 0.19 b
0.6d^{-1}	0.55 ± 0.01 c	31.7 ± 2.1 a	0.41 ± 0.24 ab
	Stress phase		
	Biomass (g L^{-1} d^{-1})	**Lipids (mg L^{-1} d^{-1})**	**Carotenoids (mg L^{-1} d^{-1})**
0.2d^{-1}	0.43 ± 0.01 a	69.9 ± 4.7 a	1.04 ± 0.15 a
0.4d^{-1}	0.53 ± 0.02 b	89.0 ± 16.1 b	1.26 ± 0.17 a
0.6d^{-1}	0.35 ± 0.03 c	31.7 ± 3.5 c	0.33 ± 0.13 b

The dilution rates produced different patterns of light availability (Table 3) which were related to several effects on the biomass productivity, physiological state and biochemical composition of the biomass. Low dilution rates generated conditions of lower light and nutrient availability than high dilution rates. The dilution rates of 0.2 d^{-1} and 0.8 d^{-1} reached a daily mean E_{av} of 56 µmol photons m^{-2} s^{-1}, and 653 µmol photons m^{-2} s^{-1} respectively (Figure S1, supplementary material). According to the values obtained for the onset of irradiance saturating photosynthesis (E_{kPSII}, Table

3), it is likely that the cultures were mainly photo-limited in low dilution rate (0.2 d^{-1}), and on the contrary, at high dilution rates the cultures were close to photosaturation (0.6 d^{-1}). Thus, it is very helpful to model the growth rate of the strain as a function of the average irradiance inside the culture, since these models are an essential tool for optimizing the operation, as well as for the scale up [35]. Molina-Grima et al. [20] proposed a hyperbolic function to describe the relationship between the growth rate and average irradiance (Eq. 4). Fitting the steady-state data (last 3 days) by nonlinear regression (Figure S2, supplementary material), the parameters obtained were μ_{max} = 0.85 d^{-1}, E_k = 97.9 µmol photons m^{-2} s^{-1}, and n = 1.4 (r^2 = 0.9663) which agree with the previously referenced μ_{max} (0.78 d^{-1}, [15]). The optimum dilution rate and daily mean E_{av} obtained by simulation of the model (Figure S3 supplementary material) should be close to D = 0.395 d^{-1} and 88.4 µmol photons m^{-2} s^{-1} which is in concordance with the maximum biomass productivity and E_{av} obtained at the dilution rate of 0.4 d^{-1} (Table 2 and 3). The expected E_{av} in an outdoor photobioreactor can be obtained by a correct photobiorreactor design and culture operation mode [36]. The value of E_k is close to those obtained for other strains as *H. pluvialis* E_k = 99 µmol photons m^{-2} s^{-1} [37], *I. galbana* E_k = 130 µmol photons m^{-2} s^{-1} [20] and *Phaeodactylum tricornutum* E_k = 116 µmol photons m^{-2} s^{-1} [38].

The growth of microalgae is determined by the photosynthesis rate, which is a direct function of the irradiance to which the cells are exposed inside the culture. However, excess of light can damage the photosynthetic apparatus. The maximum quantum yield of PSII (Fv/Fm) is often used as an indicator of physiological status and photoinhibition [39,40]. High values of Fv/Fm were observed in the dilution rates of 0.2, 0.4 and 0.6 d^{-1} along semicontinuous culture (Figure 3A) which indicates a

good state of the photosynthetic apparatus. The dilution rate 0.8 d^{-1} presented a decrease of Fv/Fm from the day 6 (Figure 3A). This decrease can be due to the increase in the E_{av} (Figure S1, supplementary material) which can lead to a photoinhibition and stress process. Interestingly, a significant reduction of Fv/Fm in dependence of the previous dilution rate was observed at first day under salinity stress (Figure 3A). Then, a recovery of the value Fv/Fm was observed for all cultures on day 6 of stress (Figure 3A). Figure 3B shows the correlation of Fv/Fm with the E_{av} using the data of culture stage I. Drastic decrease in the value of Fv/Fm was observed above a daily mean E_{av} of 570 µmol photons m^{-2} s^{-1} (dashed line in Figure 3B). Therefore, that daily mean E_{av} value can be taken as a threshold to avoid a photoinhibition process in cultures of *Golenkinia* FAUBA-3.

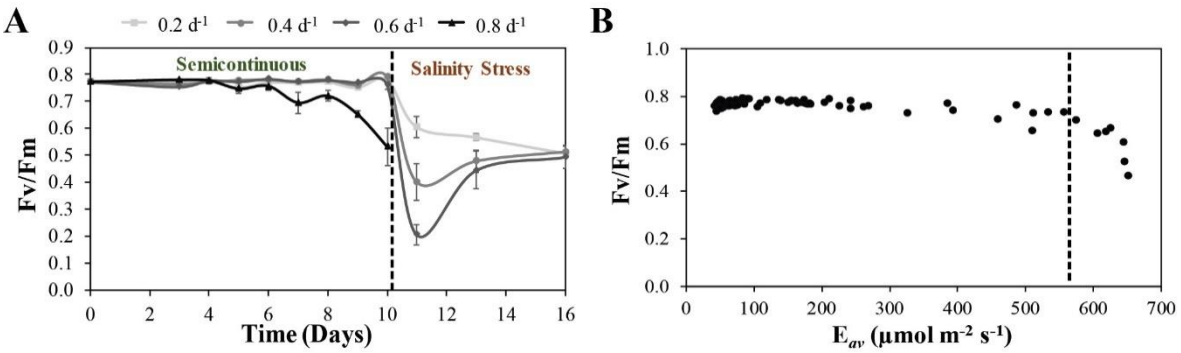

Figure 3. Maximum quantum yield of PSII (Fv/Fm**). (A)** Time course of Fv/Fm under semicontinuous cultures (0.2, 0.4, 0.6 and 0.8 d^{-1} dilution rates) and batch salinity stress**. (B)** Correlation between Fv/Fm and the daily mean E_{av} (the vertical dashed line corresponds to a photosynthetic threshold) of *Golenkinia* FAUBA-3.

In addition, photosynthesis measurement performed by P vs E curves (Table 3) is more descriptive of the whole photosynthetic process than Fv/Fm since they involve all the cell physiology. The best photosynthetic performance expressed on Chl basis was obtained at 0.2 d^{-1} dilution rate which showed the highest photosynthetic efficiency (initial slope of ETR* vs. E_{PAR}; α*) and maximum electron transport rate (ETR**max*) (Table 3). Nevertheless, no significant differences were observed in the photosynthetic productivity on dry weight basis (ETR_B*max*) between all dilution rates (Table 3), but the 0.4 d^{-1} dilution rate showed a tendency of higher values which is in concordance with its higher biomass productivity (Table 2). The opposite behavior of ETR*max* expressed on Chl basis (ETR**max*) and dry weight basis (ETR_B*max*) (Table 3) can be explained due to the differences observed in the Chl content of the cells which affected the optical properties of the cultures (*i.e. in vivo* chlorophyll absorption cross-section [a*; m^2 mg Chl^{-1}] and biomass extinction coefficient [Ka; m^2 gDW^{-1}]). The chlorophyll content was 0.83, 4.38, and 3.06 mg g DW^{-1} in the cultures at 0.2, 0.4 and 0.6 d^{-1} dilution rates respectively. The treatment 0.4 d^{-1} with the highest value of Chl content showed the lowest a* and the highest Ka, which entails an opposite behavior of ETR**max* and ETR_B*max* according to its calculation (Eq. 5 and 6 respectively). Similar behavior was observed in the photosynthesis parameters elaborated on a chlorophyll and cell basis in *Nannochloropsis* species exposed to different light intensities [41]. These results indicate an adaptation of the overall photosynthetic apparatus to the different steady-state conditions (light and nutrients regime) which led to different photosynthetic performance. Therefore, the highest biomass productivity of the culture at 0.4 d^{-1}

dilution rate can be explained since the cells showed the highest photosynthetic performance on biomass basis and were exposed to an optimal irradiance regime.

Table 3. Photosynthetic performance and optical properties of *Golenkinia* FAUBA-3 under semicontinuous cultures at steady-state condition and salinity stress. E_{av} = daily mean average irradiance inside the culture; Ka = biomass extinction coefficient; a* = *in vivo* chlorophyll absorption cross section; α * = initial slope of ETR* vs. PAR; $ETR^{*}max$ = maximum electron transport rate by chlorophyll unit; $ETR_{B}max$ = maximum electron transport rate by biomass unit; $E_{k\ PSII}$ = onset of irradiance saturating photosynthesis; $E_{opt\ PSII}$ = irradiance of the initial photoinhibition; NPQ*max* = maximum non-photochemical quenching. Data are the means and standard deviation of three replicate experiments. Different letters indicate significant differences of means ($p<0.05$).

	Semincontinuous cultures		
	0.2 d^{-1}	**0.4 d^{-1}**	**0.6 d^{-1}**
E*av* (μmol photons m^{-2} s^{-1})	56.5 ± 5.6 a	83.1 ± 4.9 a	260.3 ± 99.9 b
Ka (m^2 g DW^{-1})	0.13 ± 0.01 a	0.15 ± 0.02 a	0.13 ± 0.06 a
a* (m^2 mg Chl^{-1})	0.085 ± 0.006 a	0.018 ± 0.002 b	0.041 ± 0.002 c
α *	0.026 ± 3.E-04 a	0.005 ± 1.E-04 b	0.011 ± 5.E-04 c

ETR*max* (µmol e^- mg $Chla^{-1}$ s^{-1})	4.30	±	0.40	a	1.09	±	0.19	b	2.32	±	0.13	c
ETR_B*max* (µmol e^- g DW^{-1} s^{-1})	6.55	±	1.04	a	8.67	±	1.43	a	7.70	±	3.83	a
$E_{k\ PSII}$ (µmol photons m^{-2} s^{-1})	166.7	±	16.6	a	205.5	±	38.2	a	212.2	±	18.1	a
$E_{opt\ PSII}$ (µmol photons m^{-2} s^{-1})	1204.5	±	76.8	a	2141.0	±	610.0	b	1108.2	±	91.2	a
NPQ*max*	0.91	±	0.12	a	0.78	±	0.01	a	0.74	±	0.02	a

	Stress phase											
	0.2 d^{-1}				**0.4 d^{-1}**				**0.6 d^{-1}**			
E*av* (µmol photons m^{-2} s^{-1})	149.4	±	31.1	a	252.7	±	7.7	a	413.5	±	48.8	b
Ka (m^2 g DW^{-1})	0.08	±	0.02	a	0.07	±	0.00	a	0.07	±	0.01	a
a* (m^2 mg Chl^{-1})	0.032	±	0.008	ab	0.027	±	0.002	a	0.044	±	0.005	ab

α *	0.002	±	2.E-03	a	0.002	±	6.E-04	a	0.001	±	1.E-04	a
ETR*max (µmol e^- mg $Chla^{-1}$ s^{-1})	0.29	±	0.13	a	0.61	±	0.20	a	0.25	±	0.05	a
$ETR_B max$ (µmol e^- g DW^{-1} s^{-1})	1.02	±	0.47	a	0.96	±	0.06	a	0.47	±	0.03	a
$E_{k\ PSII}$ (µmol photons m^{-2} s^{-1})	116.0	±	49.2	a	433.4	±	240.4	ab	332.3	±	32.0	b
$E_{opt\ PSII}$ (µmol photons m^{-2} s^{-1})	----	±	----	a	----	±	----	b	738.7	±	65.5	a
NPQmax	0.39	±	0.09	a	0.29	±	0.03	ab	0.12	±	0.03	b

Under salinity stress in batch mode a drastic decrease was observed in all photosynthetic parameters (Table 3) which indicate a widespread photodamage or a controlled process of dismantling of the photosynthetic apparatus [42]. The latest case is expected, since it was reported a resistant cell stage (halotolerant aplanospore) under salinity stress that after a re-suspension in fresh medium can recovery rapidly [15]. In addition, a higher dispersion of the RLC data under the stress phase was observed which can be explained by a reduced cell fluorescence emission, and therefore a high ratio of noise/signal of the device can increase dispersion of the data.

The interference between nutrient status and light intensity has already been reported in biomass production and carotenogenesis studies [43–46]. In the case of the dilution rate of 0.2 d^{-1}, nitrogen could be another limiting factor beside light at steady-state condition, since it was observed almost total depletion of $N\text{-}NO_3^-$ (Figure 4). In addition, the E_{av} was lower than both the onset of irradiance saturating photosynthesis (E_{kPSII}, Table 3) and the optimum E_{av} obtained by the growth model (E_k). The nitrogen deficiency could explain the lowest Chl content of the biomass and highest NPQ*max* at 0.2 d^{-1} dilution rate. On the other hand, the 0.6 d^{-1} dilution rate presented full nutrient availability (Figure 4) and higher average irradiance inside the culture (E_{av}) than E_{kPSII} (Table 3). Phosphorus showed no considerable differences between treatments at steady-state condition (Figure 4).

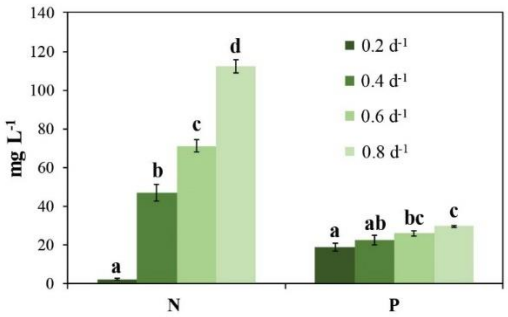

Figure 4. Nitrogen and phosphorus concentration at steady-state condition in the different dilution rates under semicontinuous cultures of *Golenkinia* FAUBA-3. Data are the means and standard deviation of three replicate experiments. Different letters indicate significant differences of means ($p<0.05$).

3.2. Biochemical characterization: lipid and carotenoid productivity

It has been widely reported that microalgae change their biochemical composition in response to different nutrient and light regimes [16]. Figure 5 shows the biochemical composition of the biomass under the first and second culture stages. In the semicontinuous cultures the carbohydrate and protein content showed an opposite response to the dilution rate (Figure 5A). As expected, in cultures with low nutrient availability (0.2 d^{-1}) we observed higher carbohydrate and lower protein content [34]. It was reported in several microalgae species that under low nutrient availability the carbon allocation is mainly destined to accumulate energy and carbon reserves, as carbohydrates, and a deprivation of protein synthesis [47,48]. The change of the dilution rate from 0.2 d^{-1} to 0.6 d^{-1} produced a 39 % reduction in carbohydrate content and 75 % increase of protein content of the biomass. This is interesting because it would be possible to control the biochemical composition of the biomass for different biorefinery products as function of dilution rates. On the contrary, lipid content did not show relevant changes among different dilution rates under semicontinuous mode ranging around 5.3 and 8 % DW (Figure 5A). Nevertheless, the lipid content was lower than the obtained at stationary-phase under batch mode in JM media (21.3 % lipids DW) [15]. This can be explained due to the lower nutrient concentration of JM than Arnon media and the different operation mode of the cultures.

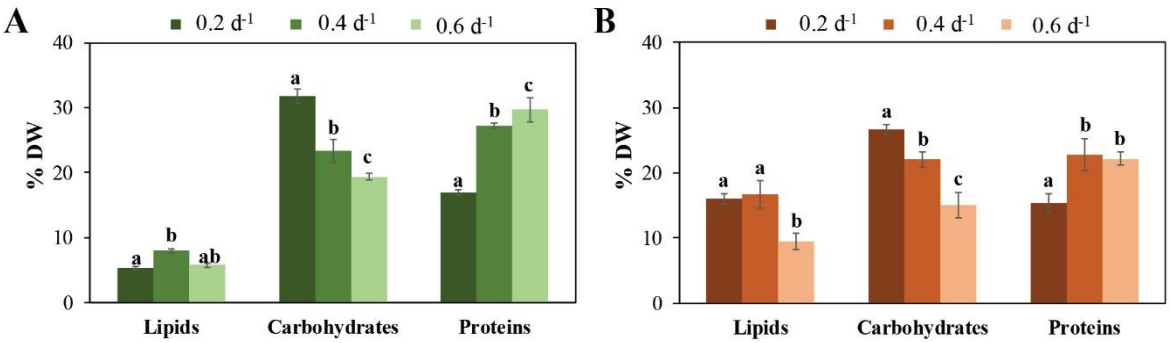

Figure 5. Biochemical composition of *Golenkinia* FAUBA-3 expressed as percentage of dry weigh obtained by different dilution rate under semicontinuous cultures at steady-state condition (A) and under salinity stress (B). Data are the means and standard deviation of three replicate experiments. Different letters indicate significant differences of means ($p<0.05$).

Under salinity stress carbohydrate and protein content kept their tendency regarding the different dilution rates, but a decrease on both was observed at the expense of lipid accumulation after stress period (Figure 5A and 5B). The lipid content was around 16.1 %, 16.7 %, and 9.5 % DW (Figure 6B) under 0.2, 0.4, and 0.6 d^{-1} dilution rate respectively which was similar to the values obtained by Usmani et al. [49] but lower than the lipid content obtained after a long batch culture and stress period reported by Rearte et al. [15] and Nie et al. [50] for *Golenkinia* strains. The accumulation of carbohydrates and lipids would function mainly as reserves of carbon and energy, among other possible roles [48,51]. In general, under nutrient depletion or stress conditions carbohydrates is synthetized prior to lipid which has been widely reported (for a review, see [47], and references there in). Some reports indicate that the carbohydrates, accumulated in the short-term starvation, are degraded to support the subsequent lipid biosynthesis in the long-term stress

[48,52,53]. Since the photosynthetic activity of *Golenkinia* FAUBA-3 was dramatically reduced under salinity stress period (Table 3), it was expected that the carbon necessary for the lipid biosynthesis probably come from carbohydrate degradation.

The increase of lipid accumulation after stress period varied on each previous dilution rate treatment: an increase of 201 %, 110 %, and 64 % in the dilution rates of 0.2, 0.4, and 0.6 d^{-1} was observed respectively. Those results demonstrate that the magnitude of lipid accumulation rate under salinity stress was dependent on the previous physiological state of the culture. The culture with the lowest dilution rate was acclimated to low nutrient and light availability and probably a major activity of the secondary metabolism had effect on lipid accumulation. At this point, it is important to consider that the previous physiological state of the cells to any drastic stress will determine the survival success, since it is necessary a whole reorientation of the metabolism to generate a resistant stage. If those changes cannot be performed faster than the stress process, the survival success of the cells will decrease. Furthermore, the accumulation of secondary metabolites under stress conditions requires time which is a key factor in any biotechnological production process. This time can be reduced if the cells have active the secondary metabolism before the stress period.

The fatty acids profiles are shown in Table 3. Palmitic (c16:0), oleic (c18:1n-9), linoleic (c18:2n-6), and alpha-linolenic (ALA, c18:3n-3) acids represented around 84 % of total FAMEs in all conditions. Nie et al. [50] showed a similar FAMEs composition in a strain of *Golenkinia* SDEC-16., but the proportion of palmitic and ALA are higher and lower respectively than the strain *Golenkinia* FAUBA-3.

Semicontinuous cultures presented the highest content of PUFAs which ranged between 47-52 % of total FAMEs, composed mostly of linoleic and ALA acids. At high dilution rates, it was observed an increase of ALA at the expense of oleic and linoleic decrease. ALA is an essential ω3 long-chain polyunsaturated fatty acid (ω3 LC-PUFA) with an important nutritional role in mammals, and humans in particular [1], and it is the dietary precursor for the ω3 LC-PUFAs eicopentaenoic (EPA, 20:5n-3), docosapentaenoic acid (DPA, 22:5n-3) and docosahexaenoic acid (DHA, 22:6n-3) [54]. Under salinity stress the proportion of MUFAs increased (c18:1n-9) and the proportion of PUFAs decreased (c18:2n-6 and c18:3n-3) which resulted in a balanced composition of SFAs, MUFAs and PUFAs. The higher PUFAs content under semicontinuous culture can be explained since they are crucial for regulating the membrane structure, fluidity, phase transitions and permeability associated to an active cell division and growth [55]. The higher content of MUFAs and SFA under salinity stress could be explained since they are a more stable storage of carbon and energy than PUFAs. PUFAs also act as the precursors of many metabolites that regulate vital biological growth functions that can be suppressed in a cell resistant stage. The main source of ω3 PUFAs is fish oils and certain vegetables, but due to the problems concerning fish oil (contamination, decrease of fish stocks, and organoleptic issues), it is crucial to produce alternative sources of ω3 as in the case of this strain of *Golenkinia* FAUBA-3.

Figure 6 shows the content of total carotenoid under semicontinuous culture and batch stress. The major accumulation of total carotenoid under salinity stress was observed at the dilution rates of 0.2 and 0.4 d^{-1} which was around 2.4 mg g^{-1} DW (Figure 6A). Rearte et al. [15] reported similar values of total carotenoid in *Golenkinia*

FAUBA-3 (2.1 mg g^{-1} DW) but it was obtained after 16 days of salinity stress period performed with ½ sea water (17.5 g L^{-1}). In this study, the salinity stress was conducted by adding marine salt to a final concentration of 35g L^{-1} which can explain the faster accumulation of carotenoid.

Table 3. Fatty acid profiles of *Golenkinia* FAUBA- 3 under semicontinuous cultures at steady-state condition and salinity stress at different dilution rates detected by GC-FID. Values are given as percentages of total FAMEs. Data are the means and standard deviation of three replicate experiments. Different letters indicate significant differences of means ($p<0.05$). SFAs = Saturated Fatty Acids; MUFAs = Monounsaturated Fatty Acids; PUFAs = Polyunsaturated Fatty Acids. The main fatty acids are highlighted in gray.

	Semicontinuos			**Stress**		
	0.2 d^{-1}	**0.4 d^{-1}**	**0.6 d^{-1}**	**0.2 d^{-1}**	**0.4 d^{-1}**	**0.6 d^{-1}**
C14:0	0.2 ± 0.0	0.2 ± 0.0	0.3 ± 0.0	0.4 ± 0.0	0.3 ± 0.2	0.3 ± 0.0
C14:1	0.5 ± 0.1	0.3 ± 0.4	1.0 ± 0.2	0.1 ± 0.0	0.0 ± 0.0	0.2 ± 0.1
C16:0	**25.1 ± 1.1**	**23.4 ± 1.6**	**27.0 ± 0.9**	**21.2 ± 0.1**	**26.2 ± 6.4**	**25.9 ± 3.7**
C16:1	0.4 ± 0.1	0.6 ± 0.0	1.4 ± 0.4	0.1 ± 0.0	0.1 ± 0.1	0.3 ± 0.1
C17:0	7.8 ± 0.8	9.4 ± 0.2	4.8 ± 0.5	8.0 ± 0.1	8.2 ± 2.4	5.4 ± 0.9
C18:0	3.6 ± 1.6	5.0 ± 0.5	6.5 ± 0.7	3.7 ± 0.0	3.0 ± 1.2	3.8 ± 0.3
C18:1n9c	**12.1 ± 0.8**	**6.8 ± 0.0**	**6.5 ± 0.3**	**35.3 ± 0.8**	**29.7 ± 8.9**	**33.4 ± 2.4**
C18:2n6c	**33.4 ± 1.2**	**35.5 ± 0.2**	**26.3 ± 0.5**	**23.0 ± 0.5**	**22.3 ± 1.1**	**19.3 ± 1.4**
C18:3n6	0.2 ± 0.0	0.1 ± 0.0	0.1 ± 0.0	0.2 ± 0.0	0.1 ± 0.1	0.4 ± 0.1
C18:3n3	**13.3 ± 0.4**	**16.3 ± 1.1**	**23.9 ± 0.6**	**5.2 ± 0.1**	**8.2 ± 2.4**	**7.7 ± 0.3**
C20:0	0.7 ± 0.0	0.4 ± 0.0	0.3 ± 0.0	0.9 ± 0.1	0.5 ± 0.5	0.7 ± 0.0
C20:1	0.3 ± 0.0	0.2 ± 0.0	0.2 ± 0.0	0.6 ± 0.0	0.5 ± 0.5	0.9 ± 0.0

C22:0	0.8	±	0.0		0.4	±	0.0		0.4	±	0.1		0.6	±	0.1		0.4	±	0.3		0.5	±	0.1	
C22:1n9	0.6	±	0.2		0.8	±	0.0		0.6	±	0.3		0.2	±	0.0		0.1	±	0.1		0.7	±	0.5	
C24:0	0.2	±	0.0		0.1	±	0.0		0.1	±	0.0		0.2	±	0.0		0.1	±	0.1		0.1	±	0.0	
SFAs	**38.7**	**±**	**1.1**	**a**	**39.1**	**±**	**1.4**	**a**	**39.6**	**±**	**1.1**	**a**	**35.1**	**±**	**0.2**	**a**	**38.8**	**±**	**6.3**	**a**	**36.9**	**±**	**3.2**	**a**
MUFAs	**14.0**	**±**	**0.6**	**a**	**8.7**	**±**	**0.4**	**b**	**9.7**	**±**	**0.6**	**b**	**36.4**	**±**	**0.8**	**b**	**30.5**	**±**	**9.7**	**b**	**35.6**	**±**	**1.7**	**b**
PUFAs	**47.3**	**±**	**1.1**	**a**	**52.2**	**±**	**1.0**	**b**	**50.7**	**±**	**0.9**	**ab**	**28.4**	**±**	**0.6**	**c**	**30.7**	**±**	**3.4**	**c**	**27.5**	**±**	**1.6**	**c**

The increase of carotenoid accumulation after stress period was 998, 217, and 91 % for the dilution rates of 0.2, 0.4, and 0.6 d^{-1} respectively compared to the carotenoid content under semicontinuous operation at steady-state condition. These results indicate that nutrient deprivation in lower dilution rates could have overstimulated the accumulation of carotenoid under salinity stress period. The functions of secondary carotenoids (not coupled to the photosynthetic apparatus) accumulated during stress would be associated with a passive photoprotection since they act as a radiation filter [56] and exhibit antioxidant activity [57]. The carotenoid accumulation showed a similar response on lipids. This supports the evidence that coordinated carotenoid and lipid synthesis under different stress types where intracellular oil droplets serve as host for the produced carotenoids [15,58,59]. A high NPQ (Non-Photochemical Quenching of chlorophyll fluorescence) value indicates high photoprotection activity since it is a measure of the capacity to dissipate the excess of absorbed light [3]. NPQ values under salinity stress (Table 3) were high at low dilution rate in which the carotenoid accumulation was higher. Lutein, β-carotene and astaxanthin were the main carotenoid identified in a decreasing order (Figure 7B). Lutein and β-carotene are widely present in the class Chlorophyceae and

astaxanthin is present in some Chlorophyceae such as *H. pluvialis* and *Chlorella zofingiensis* [60]. Currently, only *D. salina* and *H. pluvialis* are commercially produced for β-carotene (0.7 – 13 mg L^{-1} d^{-1}) and astaxanthin (0.44 - 8 mg L^{-1} d^{-1}) respectively [4,61]. Lutein is produced from Marigold oleoresin which has high land requirements and low productivities compared to microalgae data reports [62].

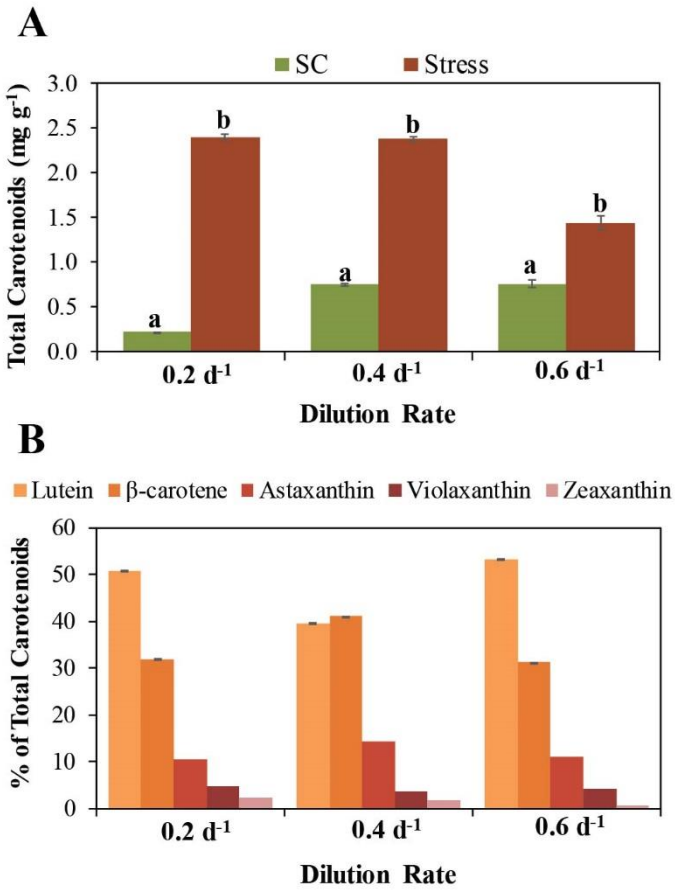

Figure 6. Total carotenoid content (mg g DW^{-1}) under semicontinuous (SC) cultures at steady-state condition and salinity stress (A) and relative carotenoid composition expressed as percentages (%) of total carotenoids identified by HPLC-DAD (B). Data are the means and standard deviation of three replicate experiments. Different letters indicate significant differences of means ($p<0.05$). Carotenoid composition was determined with a composed sample of the three replicates.

The productivity of a desired compound is one the most important parameters that determine the biotechnological potential for commercial purposes of any microalgae strain. The highest productivity of lipid (89 mg L^{-1} d^{-1}) and carotenoid (1.26 mg L^{-1} d^{-1}) was obtained under a dilution rate of 0.4 d^{-1} coupled to salinity stress (Table 2). Note that although the biomass productivity decreased under salinity stress, the carotenoid productivity was increased by coupling the stress phase to the 0.4 d^{-1} dilution rate (261 % compared to one-stage culture). This was explained by the increased carotenoid accumulation. Those results confirm that two-stage culture is an adequate strategy to optimize carotenoid and lipid productivity of the strain *Golenkinia* FAUBA-3. This implies a first culture stage to maximize biomass productivity under semicontinuous culture, followed by a second culture stage under high salinity stress to induce carotenoid and lipid accumulation. The lipid productivity of *Golenkinia* FAUBA-3 was higher than those reported by Ra et al. [63] and Xia et al. [64] who have performed two-stage cultures coupled with salt stress for lipid production ranging from 14 to 61 mg L^{-1} d^{-1} by different microalgae strains. Recently, Bermejo et al. [11] reported an enhanced productivity of lipid (101.7 mg L^{-1} d^{-1}) and carotenoid (1.82 mg L^{-1} d^{-1}; lutein + β-carotene) by salt stress (100 mM NaCl) in a new strain of *Coccomyxa onubensis* which is slightly higher than the productivity obtained in this study (Table 2). Interestingly, Nie et al. [50] reported a robust strain of *Golenkinia* SDEC-16 which was able to grow in sewage and BG-11 medium but with lower lipid productivity (between 15.3 and 43.4 mg L^{-1} d^{-1}). In addition, *Golenkinia* SDEC-16 strain presented good sedimentation properties due to large cell volume that could facilitate the harvesting process [50]. On the other hand, other

studies evaluated a simultaneous one step production of triacylglycerol and astaxanthin from *Chlorella zofingiensis* and *H. pluvialis* using semi-continuous cultures with nitrogen limitation obtaining high levels of productivity [61,65]. According to few studies published about *Golenkinia* strains, new experiences are necessary to study the effects of the interaction of the gradients of salinity, light, and nutritional state of the biomass to optimize accumulation rate of lipids and carotenoids and shorten the stress period. High coupled productivity of lipids and carotenoids and its profiles of fatty acids and carotenoid composition could promote the application of the biomass of *Golenkinia* FAUBA-3 in the nutraceutical and aquaculture feed fields [66]. In this context, new regulations to use new microalgae species in human food and animal feed should be considered.

According to the results obtained in this study, the general process to couple daily biomass production under semicontinuous mode operation with a batch stress phase to produce rich lipid-carotenoid biomass of *Golenkinia* FAUBA-3 should follow the scheme proposed in the Figure 8. The first stage culture should be carried out under semi-continuous cultures in controlled closed photobiorreactors (PBR-1), such as flat panels or tubular PBRs, where the daily biomass produced should be concentrated (*e.g.* membrane filtration or flotation) and re-suspended in seawater for six days in a new photobioreactor (PBR-2), as thin layer cascades for optimum light exposition. It should be necessary six PBRs in the second culture stage (one for each biomass harvested every day of the culture stage I) for reach the time necessary for accumulation. On day six the PBR-2 of the scheme must be harvested completely and it would be available for a new batch stress period. On day 7 the PBR-3 must be harvested completely and it would be available for a new batch stress

period, and in the same way on the following days. Therefore, we can obtain a daily stressed biomass production coupled to the semicontinuous culture. Nevertheless, with new studies of stress optimization, the time for carotenoid and lipid accumulation could be shortened and therefore a smaller amount of PBR for the stress phase would be necessary.

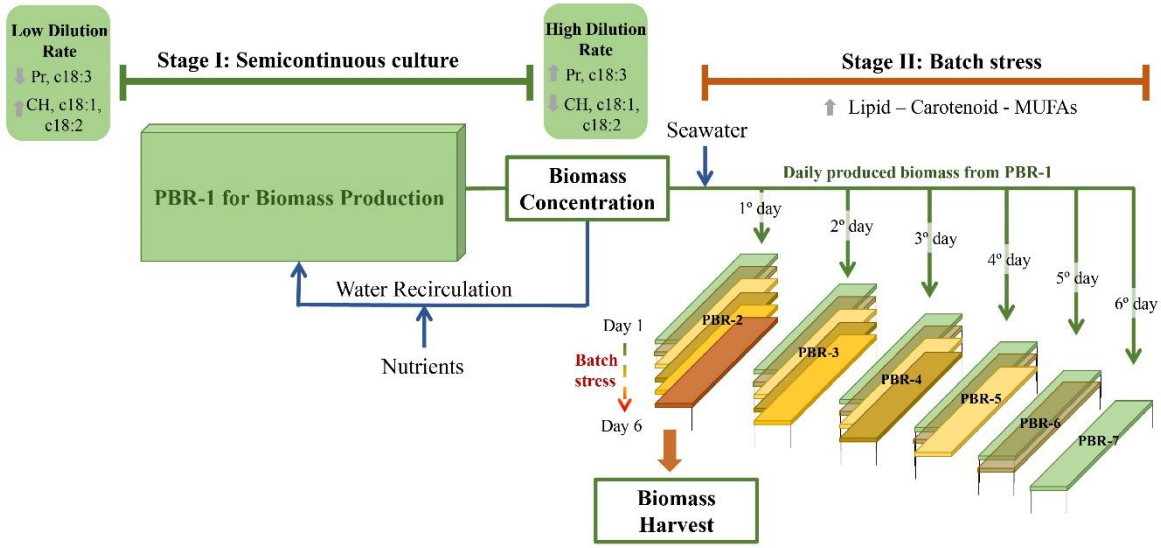

Figure 7. Summary of the biotechnological process to produce carotenoids and lipids from *Golenkinia* FAUBA-3 employing a two-stage culture system. At steady-state condition the biomass harvested from PBR-1 must be transferred to a new photobioreactor for the batch stress. Since, the batch stress takes 6 days, there are necessary six PBRs for the biomass harvested daily from PBR-1. On day 6 the PBR-2 must be harvested completely and it would be available for a new batch stress period. On day 7 the PBR-3 must be harvested completely and it would be available for a new batch stress period, and in the same way on the following days. Pr = Protein; CH = Carbohydrate; MUFAs = Monounsaturated Fatty Acids; c18:1 = oleic acid; c18:2 = linoleic acid; c18:3 = alpha-linolenic acid; PBR= Photobioreactor; 1º day to 6º day = it is the beginning of a new stress phase for a culture

transferred from PBR-1 to a new PBR; Day 1 to Day 6 = time of stress for lipids and carotenoid accumulation of one PBR.

4. Conclusions

Two-stage cultivation system was evaluated for the co-production of lipid and carotenoid in the strain *Golenkinia* FAUBA-3. In a first step, the biomass productivity was improved up to 0.92 g L^{-1} d^{-1} under semicontinuous culture with a dilution rate of 0.4 d^{-1}. The experimental data correlated well to the model of specific growth rate as function of E_{av} and we obtained the optimum dilution rate (0.395 d^{-1}) and optimum daily mean E_{av} (88.4 µmol photons m^{-2} s^{-1}). These results are very helpful for the scale up and photobioreactor design. The maximum dilution rate for this strain should be lower than 0.8 d^{-1} due to washing-out of the biomass was observed. Both photosynthetic response and biomass composition showed an adaptation to the different steady-state conditions under semicontinuous cultures. In the second stage, an increase of salinity in batch mode induced lipid and carotenoid accumulation. The main carotenoid identified were lutein, β-carotene and astaxanthin in a decreasing order. The highest productivity of lipid (89 mg L^{-1} d^{-1}) and carotenoid (1.26 mg L^{-1} d^{-1}) was obtained under salinity stress coupled to a semicontinuous culture at a dilution rate of 0.4 d^{-1}. Those results confirm that two-stage culture is an adequate strategy for optimizing carotenoid and lipid productivity in the strain *Golenkinia* FAUBA-3 which offers a great biotechnological potential. New studies are necessary to study the interaction of gradients of salinity, light, and

nutritional state of the biomass to optimize the lipid and carotenoid accumulation rate.

5. Acknowledgments

This paper is a contribution of the Research Institute of Blue Biotechnology and Development (IBYDA- Malaga University), the European Union's Horizon 2020 Research and Innovation program under the Grant Agreement No. 727874, the Agencia Nacional de Promoción Científica y Tecnológica, Argentina, (project PICT 2012- 2837), the Universidad de Buenos Aires (Facultad de Agronomía and Facultad de Ciencias Exactas y Naturales), Argentina, and the Instituto de Micología y Botánica (INMIBO), Consejo Nacional de Investigaciones Científicas y Técnicas (CONICET), Argentina. Thanks to the Argentinian Government through the Bec.AR program.

6. Author contributions

Rearte T.A. (tarearte@agro.uba.ar) has contributed to the design of experiments and has led the laboratory work, analysis, interpretation of the data and drafting of the manuscript. **Figueroa F.L**. (felix_lopez@uma.es) and **Acién F.G.** (facien@ual.es) has contributed in the direction and design of experiments, interpretation of the data and critical revision of the manuscript and data processing. **Gómez-Serrano C.** (cinti4201@hotmail.com) and **Marsili S.** (santiagonicolasmarsili@gmail.com) has contributed to the laboratory work, analysis, and interpretation of the data. **Vélez C.G.** (memov2007@gmail.com) and **Iorio de F.A.** (aiorio@agro.uba.ar) has contributed to the interpretation of the data

and critical revision of the manuscript. **Cerón-García M.C.** (mcceron@ual.es), **González-López, C.V** (cgl665@ual.es) and **Abdala R.** (abdala@uma.es) has contributed to the biochemical analysis, GC and HPLC methods and critical revision of the manuscript. All authors read and approved the final manuscript.

7. References

[1] E. Abedi, M.A. Sahari, Long-chain polyunsaturated fatty acid sources and evaluation of their nutritional and functional properties, Food Sci. Nutr. 2 (2014) 443–463. https://doi.org/10.1002/fsn3.121.

[2] R. Sathasivam, J.S. Ki, A review of the biological activities of microalgal carotenoids and their potential use in healthcare and cosmetic industries, Mar. Drugs. 16 (2018) 1–31. https://doi.org/10.3390/md16010026.

[3] C. Faraloni, G. Torzillo, Synthesis of Antioxidant Carotenoids in Microalgae in Response to Physiological Stress, in: D. Cvetkovic, G. Nikolic (Eds.), Carotenoids, IntechOpen, 2017: pp. 143–157. https://doi.org/10.5772/65523.

[4] R.R. Ambati, D. Gogisetty, R.G. Aswathanarayana, S. Ravi, P.N. Bikkina, L. Bo, S. Yuepeng, Industrial potential of carotenoid pigments from microalgae: Current trends and future prospects, Crit. Rev. Food Sci. Nutr. 59 (2019) 1880–1902. https://doi.org/10.1080/10408398.2018.1432561.

[5] K. Rajesh, M. V. Rohit, S. Venkata Mohan, Microalgae-Based Carotenoids Production, in: Algal Green Chem. Recent Prog. Biotechnol., 2017: pp. 139–147. https://doi.org/10.1016/B978-0-444-63784-0.00007-2.

[6] R. Liu, T. Wang, B. Zhang, L. Qin, C. Wu, Q. Li, L. Ma, Lutein and zeaxanthin supplementation and association with visual function in age-related macular

degeneration, Investig. Ophthalmol. Vis. Sci. 56 (2015) 252–258. https://doi.org/10.1167/iovs.14-15553.

[7] J. Wu, E. Cho, W.C. Willett, S.M. Sastry, D.A. Schaumberg, Intakes of lutein, zeaxanthin, and other carotenoids and age-related macular degeneration during 2 decades of prospective follow-up, JAMA Ophthalmol. 133 (2015) 1415–1424. https://doi.org/10.1001/jamaophthalmol.2015.3590.

[8] F.K.C. Fung, B.Y.K. Law, A.C.Y. Lo, Lutein attenuates both apoptosis and autophagy upon cobalt (II) chloride-induced hypoxia in rat Muller cells, PLoS One. 11 (2016) 1–19. https://doi.org/10.1371/journal.pone.0167828.

[9] R.L. Roberts, J. Green, B. Lewis, Lutein and zeaxanthin in eye and skin health, Clin. Dermatol. 27 (2009) 195–201. https://doi.org/10.1016/j.clindermatol.2008.01.011.

[10] F.G. Acién, E. Molina, J.M. Fernández-Sevilla, M. Barbosa, L. Gouveia, C. Sepúlveda, J. Bazaes, Z. Arbib, Economics of microalgae production, in: Microalgae-Based Biofuels Bioprod. From Feed. Cultiv. to End-Products, 2017: pp. 485–503. https://doi.org/10.1016/B978-0-08-101023-5.00020-0.

[11] E. Bermejo, M.C. Ruiz-Domínguez, M. Cuaresma, I. Vaquero, A. Ramos-Merchante, J.M. Vega, C. Vílchez, I. Garbayo, Production of lutein, and polyunsaturated fatty acids by the acidophilic eukaryotic microalga *Coccomyxa onubensis* under abiotic stress by salt or ultraviolet light, J. Biosci. Bioeng. 125 (2018) 669–675. https://doi.org/10.1016/j.jbiosc.2017.12.025.

[12] P. Singh, S. Kumari, A. Guldhe, R. Misra, I. Rawat, F. Bux, Trends and novel strategies for enhancing lipid accumulation and quality in microalgae, Renew. Sustain. Energy Rev. 55 (2016) 1–16.

https://doi.org/10.1016/j.rser.2015.11.001.

[13] R. Ma, S.R. Thomas-Hall, E.T. Chua, E. Eltanahy, M.E. Netzel, G. Netzel, Y. Lu, P.M. Schenk, LED power efficiency of biomass, fatty acid, and carotenoid production in *Nannochloropsis* microalgae, Bioresour. Technol. 252 (2018) 118–126. https://doi.org/10.1016/j.biortech.2017.12.096.

[14] P. Přibyl, J. Pilný, V. Cepák, P. Kaštánek, The role of light and nitrogen in growth and carotenoid accumulation in *Scenedesmus* sp., Algal Res. 16 (2016) 69–75. https://doi.org/10.1016/j.algal.2016.02.028.

[15] T.A. Rearte, C.G. Vélez, M. V. Beligni, F.L. Figueroa, P.I. Gómez, D. Flaig, A.F. de Iorio, Biological characterization of a strain of *Golenkinia* (Chlorophyceae) with high oil and carotenoid content induced by increased salinity, Algal Res. 33 (2018) 218–230. https://doi.org/10.1016/j.algal.2018.05.014.

[16] X.M. Sun, L.J. Ren, Q.Y. Zhao, X.J. Ji, H. Huang, Microalgae for the production of lipid and carotenoids: A review with focus on stress regulation and adaptation, Biotechnol. Biofuels. 11 (2018) 1–16. https://doi.org/10.1186/s13068-018-1275-9.

[17] M.J. Griffiths, S.T.L. Harrison, Lipid productivity as a key characteristic for choosing algal species for biodiesel production, J. Appl. Phycol. 21 (2009) 493–507. https://doi.org/10.1007/s10811-008-9392-7.

[18] D.I. Arnon, B.D. McSwain, H.Y. Tsujimoto, K. Wada, Photochemical activity and components of membrane preparations from blue-green algae. I. Coexistence of two photosystems in relation to chlorophyll a and removal of phycocyanin., Biochim. Biophys. Acta. 357 (1974) 231–245.

https://doi.org/10.1016/0005-2728(74)90063-2.

[19] C.G. Jerez, C.B. García, A. Rearte, F.L. Figueroa, Relation between light absorption measured by the quantitative filter technique and attenuation of *Chlorella fusca* cultures of different cell densities: application to estimate the absolute electron transport rate (ETR), J. Appl. Phycol. 28 (2016) 1635–1648. https://doi.org/10.1007/s10811-015-0685-3.

[20] E. Molina-Grima, F. García Camacho, J.A. Sánchez Pérez, J.M.F. Sevilla, F.G.A. Fernandez, A.C. Gomez, A Mathematical Model of Microalgal Growth in Light-Limited Chemostat Culture, J. Chem. Technol. Biotechnol. 61 (1994) 167–173.

[21] U. Schreiber, H. Hormann, C. Neubauer, C. Klughammer, Assessment of Photosystem II Photochemical Quantum Yield by Chlorophyll Fluorescence Quenching Analysis, Aust. J. Plant Physiol. 22 (1995) 209–220.

[22] G. Johnsen, E. Sakshaug, Biooptical characteristics of PSII and PSI in 33 species (13 pigment groups) of marine phytoplankton, and the relevance for pulse-amplitude-modulated and fast-repetition-rate fluorometry [1], J. Phycol. 43 (2007) 1236–1251. https://doi.org/10.1111/j.1529-8817.2007.00422.x.

[23] P.H.C. Eilers, J.C.H. Peeters, A model for the relationship between light intensity and the rate of photosynthesis in phytoplankton, Ecol. Modell. 42 (1988) 199–215. https://doi.org/10.1016/0304-3800(88)90057-9.

[24] P.S.M. Celis-Plá, B. Martínez, N. Korbee, J.M. Hall-Spencer, F.L. Figueroa, Ecophysiological responses to elevated CO2 and temperature in *Cystoseira tamariscifolia* (Phaeophyceae), Clim. Change. 142 (2017) 67–81. https://doi.org/10.1007/s10584-017-1943-y.

[25] J. Folch, M. Lees, G.H.S. Stanley, A simple method for the isolation and purification of total lipids from animal tissues, J Biol Chem. 226 (1957) 497–509. https://doi.org/10.1007/s10858-011-9570-9.

[26] R.M. McCready, J. Guggolz, V. Silviera, H.S. Owens, Determination of Starch and Amylose in Vegetables, Anal. Chem. 22 (1950) 1156–1158.

[27] I. Brányiková, B. Maršálková, J. Doucha, T. Brányik, K. Bišová, V. Zachleder, M. Vítová, Microalgae-novel highly efficient starch producers, Biotechnol. Bioeng. 108 (2011) 766–776. https://doi.org/10.1002/bit.23016.

[28] S.O. Lourenço, E. Barbarino, P.L. Lavín, U.M. Lanfer Marquez, E. Aidar, Distribution of intracellular nitrogen in marine microalgae: Calculation of new nitrogen-to-protein conversion factors, Eur. J. Phycol. 39 (2004) 17–32. https://doi.org/10.1080/0967026032000157156.

[29] A.R. Wellburn, The Spectral Determination of Chlorophylls a and b, as well as Total Carotenoids, Using Various Solvents with Spectrophotometers of Different Resolution, J. Plant Physiol. 144 (1994) 307–313. https://doi.org/10.1016/S0176-1617(11)81192-2.

[30] W.W. Christie, A simple procedure for rapid transmethylation of glycerolipids and cholesteryl esters, J. Lipid Res. 23 (1982) 1072–1075.

[31] M.C. Cerón-García, C. V. González-López, J. Camacho-Rodríguez, L. López-Rosales, F. García-Camacho, E. Molina-Grima, Maximizing carotenoid extraction from microalgae used as food additives and determined by liquid chromatography (HPLC), Food Chem. 257 (2018) 316–324. https://doi.org/10.1016/j.foodchem.2018.02.154.

[32] M.C. Cerón, I. Campos, J.F. Sánchez, F.G. Acién, E. Molina, Fernández,

Recovery of Lutein from Microalgae Biomass: Development of a Process for *Scenedesmus almeriensis* Biomass, J. Agric. Food Chem. 56 (2008) 11761–11766.

[33] J. Bermúdez, N. Rosales, C. Loreto, B. Briceño, E. Morales, Exopolysaccharide, pigment and protein production by the marine microalga *Chroomonas* sp. in semicontinuous cultures, World J. Microbiol. Biotechnol. 20 (2004) 179–183. https://doi.org/10.1023/B:WIBI.0000021754.59894.4a.

[34] A. Jebali, F.G. Acién, N. Jiménez-Ruiz, C. Gómez, J.M. Fernández-Sevilla, N. Mhiri, F. Karray, S. Sayadi, E. Molina-Grima, Evaluation of native microalgae from Tunisia using the pulse-amplitude-modulation measurement of chlorophyll fluorescence and a performance study in semi-continuous mode for biofuel production, Biotechnol. Biofuels. 12 (2019) 1–17. https://doi.org/10.1186/s13068-019-1461-4.

[35] J.F. Sánchez, J.M. Fernández-Sevilla, F.G. Acién, M.C. Cerón, J. Pérez-Parra, E. Molina-Grima, Biomass and lutein productivity of *Scenedesmus almeriensis*: Influence of irradiance, dilution rate and temperature, Appl. Microbiol. Biotechnol. 79 (2008) 719–729. https://doi.org/10.1007/s00253-008-1494-2.

[36] F.G. Acién, E. Molina, A. Reis, G. Torzillo, G.C. Zittelli, C. Sepúlveda, J. Masojídek, Photobioreactors for the production of microalgae, 2017. https://doi.org/10.1016/B978-0-08-101023-5.00001-7.

[37] M.C. García-Malea, F.G. Acién, J.M. Fernández, M.C. Cerón, E. Molina, Continuous production of green cells of *Haematococcus pluvialis:* Modeling of the irradiance effect, Enzyme Microb. Technol. 38 (2006) 981–989.

https://doi.org/10.1016/j.enzmictec.2005.08.031.

[38] F.G.A. Fernández, F.G. Camacho, J. a S. Pérez, J.M.F. Sevilla, E.M. Grima, Modeling of biomass productivity in tubular photobioreactors for microalgal cultures: Effects of dilution rate, tube diameter, and solar irradiance, Biotechnol. Bioeng. 58 (1998) 605–616. https://doi.org/10.1002/(SICI)1097-0290(19980620)58:6<605::AID-BIT6>3.0.CO;2-M.

[39] G. Krause Heinrich, P. Jahns, Non-photochemical Energy Dissipation Determined by Chlorophyll Fluorescence Quenching: Characterization and Function, in: G.C. Papageorgiou, G. Govindjee (Eds.), Chlorophyll a Fluoresc. A Signat. Photosynth., 2004: pp. 463–495.

[40] H.M. Kalaji, G. Schansker, R.J. Ladle, V. Goltsev, K. Bosa, S.I. Allakhverdiev, M. Brestic, F. Bussotti, A. Calatayud, P. Dąbrowski, N.I. Elsheery, L. Ferroni, L. Guidi, S.W. Hogewoning, A. Jajoo, A.N. Misra, S.G. Nebauer, S. Pancaldi, C. Penella, D. Poli, M. Pollastrini, Z.B. Romanowska-Duda, B. Rutkowska, J. Serôdio, K. Suresh, W. Szulc, E. Tambussi, M. Yanniccari, M. Zivcak, Frequently asked questions about in vivo chlorophyll fluorescence: Practical issues, Photosynth. Res. 122 (2014) 121–158. https://doi.org/10.1007/s11120-014-0024-6.

[41] A. Vonshak, N. Novoplansky, A.M. Silva Benavides, G. Torzillo, J. Beardall, Y.M. Palacios, Photosynthetic characterization of two *Nannochloropsis* species and its relevance to outdoor cultivation, J. Appl. Phycol. (2020) 2005–2009. https://doi.org/10.1007/s10811-019-01985-5.

[42] A. Solovchenko, O. Solovchenko, I. Khozin-Goldberg, S. Didi-Cohen, D. Pal, Z. Cohen, S. Boussiba, Probing the effects of high-light stress on pigment and

lipid metabolism in nitrogen-starving microalgae by measuring chlorophyll fluorescence transients: Studies with a δ5 desaturase mutant of *Parietochloris incisa* (Chlorophyta, Trebouxiophyceae), Algal Res. 2 (2013) 175–182. https://doi.org/10.1016/j.algal.2013.01.010.

[43] J. Fábregas, A. Domínguez, M. Regueiro, A. Maseda, A. Otero, Optimization of the culture medium for the continuous cultivation of the microalga *Haematococcus pluvialis*, Appl. Microbiol. Biotechnol. 53 (2000) 530–535. https://doi.org/10.1039/tf9676302093.

[44] E. Del Río, F.G. Acién, M.C. García-Malea, J. Rivas, E. Molina-Grima, M.G. Guerrero, Efficient one-step production of astaxanthin by the microalga *Haematococcus pluvialis* in continuous culture, Biotechnol. Bioeng. 91 (2005) 808–815. https://doi.org/10.1002/bit.20547.

[45] E. Del Río, F.G. Acién, M.C. García-Malea, J. Rivas, E. Molina-Grima, M.G. Guerrero, Efficiency assessment of the one-step production of astaxanthin by the microalga *Haematococcus pluvialis*, Biotechnol. Bioeng. 100 (2008) 397–402. https://doi.org/10.1002/bit.21770.

[46] C.G. Jerez, J.R. Malapascua, M. Sergejevová, F.L. Figueroa, J. Masojídek, Effect of Nutrient Starvation under High Irradiance on Lipid and Starch Accumulation in *Chlorella fusca* (Chlorophyta), Mar. Biotechnol. 18 (2016) 24–36. https://doi.org/10.1007/s10126-015-9664-6.

[47] W. Ran, H. Wang, Y. Liu, M. Qi, Q. Xiang, C. Yao, Y. Zhang, X. Lan, Storage of starch and lipids in microalgae: Biosynthesis and manipulation by nutrients, Bioresour. Technol. 291 (2019) 121894. https://doi.org/10.1016/j.biortech.2019.121894.

[48] X. Johnson, J. Alric, Central carbon metabolism and electron transport in *Chlamydomonas reinhardtii*: Metabolic constraints for carbon partitioning between oil and starch, Eukaryot. Cell. 12 (2013) 776–793. https://doi.org/10.1128/EC.00318-12.

[49] M.A. Usmani, M.R. Suseela, K. Toppo, S. Sheikh, S. Nayaka, Biomass nutrient profile of the green alga *Golenkinia radiata* Chodat, Int. J. Recent Adv. Multidiscip. Res. 02 (2015) 755–761. https://doi.org/10.1002/jlcr.

[50] C. Nie, H. Pei, L. Jiang, J. Cheng, F. Han, Growth of large-cell and easily-sedimentation microalgae *Golenkinia* SDEC-16 for biofuel production and campus sewage treatment, Renew. Energy. 122 (2018) 517–525. https://doi.org/10.1016/j.renene.2018.02.005.

[51] M. Vitova, K. Bisova, S. Kawano, V. Zachleder, Accumulation of energy reserves in algae: From cell cycles to biotechnological applications, Biotechnol. Adv. 33 (2015) 1204–1218. https://doi.org/10.1016/j.biotechadv.2015.04.012.

[52] G. Markou, I. Angelidaki, D. Georgakakis, Microalgal carbohydrates: an overview of the factors influencing carbohydrates production, and of main bioconversion technologies for production of biofuels, Appl. Microbiol. Biotechnol. 96 (2012) 631–645. https://doi.org/10.1007/s00253-012-4398-0.

[53] M. Garnier, G. Bougaran, M. Pavlovic, J.B. Berard, G. Carrier, A. Charrier, F. Le Grand, E. Lukomska, C. Rouxel, N. Schreiber, J.P. Cadoret, H. Rogniaux, B. Saint-Jean, Use of a lipid rich strain reveals mechanisms of nitrogen limitation and carbon partitioning in the haptophyte Tisochrysis lutea, Algal Res. 20 (2016) 229–248. https://doi.org/10.1016/j.algal.2016.10.017.

[54] J.T. Brenna, N. Salem, A.J. Sinclair, S.C. Cunnane, α-Linolenic acid supplementation and conversion to n-3 long-chain polyunsaturated fatty acids in humans, Prostaglandins Leukot. Essent. Fat. Acids. 80 (2009) 85–91. https://doi.org/10.1016/j.plefa.2009.01.004.

[55] C.Y. Yap, F. Chen, Polyunsaturated Fatty Acids: Biological Significance, Biosynthesis, and Production by Microalgae and Microalgae-Like Organisms, Algae Their Biotechnol. Potential. 2 (2001) 1–32. https://doi.org/10.1007/978-94-015-9835-4_1.

[56] J. Masojídek, G. Torzillo, J. Kopecký, M. Koblížek, L. Nidiaci, J. Komenda, A. Lukavská, A. Sacchi, Changes in chlorophyll fluorescence quenching and pigment composition in the green alga *Chlorococcum* sp. grown under nitrogen deficiency and salinity stress, J. Appl. Phycol. 12 (2000) 417–426. https://doi.org/10.1023/A:1008165900780.

[57] J.A. Del Campo, M. García-González, M.G. Guerrero, Outdoor cultivation of microalgae for carotenoid production: current state and perspectives, Appl. Microbiol. Biotechnol. 74 (2007) 1163–1174. https://doi.org/10.1007/s00253-007-0844-9.

[58] A. Solovchenko, M.N. Merzlyak, I. Khozin-Goldberg, Z. Cohen, S. Boussiba, Coordinated carotenoid and lipid syntheses induced in *Parietochloris incisa* (chlorophyta, trebouxiophyceae) mutant deficient in δ5 desaturase by nitrogen starvation and high light, J. Phycol. 46 (2010) 763–772. https://doi.org/10.1111/j.1529-8817.2010.00849.x.

[59] S. Rabbani, P. Beyer, J. v. Lintig, P. Hugueney, H. Kleinig, Induced β-Carotene Synthesis Driven by Triacylglycerol Deposition in the Unicellular Alga

Dunaliella bardawil1, Plant Physiol. 116 (1998) 1239–1248. https://doi.org/10.1104/pp.116.4.1239.

[60] S. Takaichi, Carotenoids in algae: Distributions, biosyntheses and functions of carotenoids in algae, Mar. Drugs. 9 (2011) 1101–1118. https://doi.org/10.3390/md9061101.

[61] J. Liu, X. Mao, W. Zhou, M.T. Guarnieri, Simultaneous production of triacylglycerol and high-value carotenoids by the astaxanthin-producing oleaginous green microalga *Chlorella zofingiensis*, Bioresour. Technol. 214 (2016) 319–327. https://doi.org/10.1016/j.biortech.2016.04.112.

[62] J.M. Fernández-Sevilla, F.G. Acién Fernández, E. Molina Grima, Biotechnological production of lutein and its applications, Appl. Microbiol. Biotechnol. 86 (2010) 27–40. https://doi.org/10.1007/s00253-009-2420-y.

[63] C.H. Ra, C.H. Kang, N.K. Kim, C.G. Lee, S.K. Kim, Cultivation of four microalgae for biomass and oil production using a two-stage culture strategy with salt stress, Renew. Energy. 80 (2015) 117–122. https://doi.org/10.1016/j.renene.2015.02.002.

[64] L. Xia, H. Ge, X. Zhou, D. Zhang, C. Hu, Photoautotrophic outdoor two-stage cultivation for oleaginous microalgae *Scenedesmus obtusus* XJ-15, Bioresour. Technol. 144 (2013) 261–267. https://doi.org/10.1016/j.biortech.2013.06.112.

[65] M.C. García-Malea, F. Gabriel Acién, E. Del Río, J.M. Fernández, M.C. Cerón, M.G. Guerrero, E. Molina-Grima, Production of astaxanthin by *Haematococcus pluvialis*: Taking the one-step system outdoors, Biotechnol. Bioeng. 102 (2009) 651–657. https://doi.org/10.1002/bit.22076.

[66] P. Steinrücken, S.R. Erga, S.A. Mjøs, H. Kleivdal, S.K. Prestegard,

Bioprospecting North Atlantic microalgae with fast growth and high polyunsaturated fatty acid (PUFA) content for microalgae-based technologies, Algal Res. 26 (2017) 392–401. https://doi.org/10.1016/j.algal.2017.07.030.

FIGURE LEGENDS

Figure 1. Biomass concentration of *Golenkinia* FAUBA-3under a two-stage culture system. (A) Time course of biomass concentration under semicontinuous cultures (SC) at 0.2, 0.4, 0.6 and 0.8 d^{-1} dilution rates. Different letters indicate significant differences of means between the different days in one treatment ($p<0.05$). (B) Biomass concentration at steady-state condition under semicontinuous cultures (average data from day 7 to day 10) and at final day of batch salinity stress. Data are the means and standard deviation of three replicate experiments. Different letters indicate significant differences of means between SC and stress cultures ($p<0.05$).

Figure 2. Light microscopy images of various cells of *Golenkinia* FAUBA-3 under salinity stress. (A) Completely reddish-orange cells (D = 0.4 d^{-1}) with the cell wall with bristles showing slightly plasmolysis (arrow). (B) Presence of reddish-orange-green cells (D = 0.2 d^{-1}). (C) Bleached non-viable cells (D = 0.6 d^{-1}). Scale bar 10 µm.

Figure 3. Maximum quantum yield of PSII (Fv/Fm). **(A)** Time course of Fv/Fm under semicontinuous cultures (0.2, 0.4, 0.6 and 0.8 d^{-1} dilution rates) and batch salinity stress.**(B)** Correlation between Fv/Fm and the daily mean E_{av} (the vertical dashed line corresponds to a photosynthetic threshold) of *Golenkinia* FAUBA-3.

Figure 4. Nitrogen and phosphorus concentration at steady-state condition in the different dilution rates under semicontinuous cultures of *Golenkinia* FAUBA-3. Data are the means and standard deviation of three replicate experiments. Different letters indicate significant differences of means ($p<0.05$).

Figure 5. Biochemical composition of *Golenkinia* FAUBA-3 expressed as percentage of dry weigh obtained by different dilution rate under semicontinuous cultures at steady-state condition (A) and under salinity stress (B). Data are the means and standard deviation of three replicate experiments. Different letters indicate significant differences of means ($p<0.05$).

Figure 6. Carotenoid composition of *Golenkinia* FAUBA-3. **(A)** Total carotenoid content (mg g DW^{-1}) under semicontinuous (SC) cultures at steady-state condition and salinity stress.**(B)** Relative carotenoid composition expressed as percentages (%) of total carotenoids identified by HPLC-DAD. Data are the means and standard deviation of three replicate experiments. Different letters indicate significant differences of means ($p<0.05$). Carotenoid composition was determined with a composed sample of the three replicates.

Figure 7. Summary of the biotechnological process to produce carotenoids and lipids from *Golenkinia* FAUBA-3 employing a two-stage culture system. At steady-state condition the biomass harvested from PBR-1 must be transferred to a new photobioreactor for the batch stress. Since, the batch stress takes 6 days, there are necessary six PBRs for the biomass harvested daily from PBR-1. On day 6 the PBR-2 must be harvested completely and it would be available for a new batch stress

period. On day 7 the PBR-3 must be harvested completely and it would be available for a new batch stress period, and in the same way on the following days. Pr = Protein; CH = Carbohydrate; MUFAs = Monounsaturated Fatty Acids; c18:1 = oleic acid; c18:2 = linoleic acid; c18:3 = alpha-linolenic acid; PBR= Photobioreactor; 1º day to 6º day = it is the beginning of a new stress phase for a culture transferred from PBR-1 to a new PBR; Day 1 to Day 6 = time of stress for lipids and carotenoid accumulation of one PBR.

TABLES

Table 1. Symbols and abbreviations descriptions.

Symbols	Units	Description
Ka	m^2 g DW^{-1}	Biomass extinction coefficient
a*	m^2 mg Chl^{-1}	*In vivo* chlorophyll *a*-specific absorption cross-sections of the suspension
E_{PAR}	µmol photons m^{-2} s^{-1}	Photosynthetically active irradiance
E*av*	µmol photons m^{-2} s^{-1}	Average irradiance inside the culture
µ	d^{-1}	Specific growth rate
μ_{max}	d^{-1}	Maximum specific growth rate
E_k	µmol photons m^{-2} s^{-1}	Average irradiance affinity constant of growth rate
Chl *a*		Chlorophyll a
Fv/Fm		Maximum quantum yield of PSII
RLC		Rapid Light Curve
ETR*	µmol e^- mg Chl^{-1} s^{-1}	Electron transport rate per Chl *a* unit
ETR_B	µmol e^- g DW^{-1} s^{-1}	Electron transport rate per biomass unit
α		Initial slope of ETR vs E_{PAR}
NPQ		Non photochemical quenching
$E_{k\ PSII}$	µmol photons m^{-2} s^{-1}	Onset of irradiance saturating photosynthesis

$E_{opt\ PSII}$	µmol photons m^{-2} s^{-1}	Irradiance of the initial photoinhibition

Table 2. Volumetric productivity of biomass, lipid and carotenoid of *Golenkinia* FAUBA-3 under semicontinuous cultures at steady-state condition under different dilution rates and salinity stress. Data are the means and standard deviation of three replicate experiments. Different letters indicate significant differences of means ($p<0.05$).

	Semicontinuous cultures		
	Biomass (g L^{-1} d^{-1})	**Lipids (mg L^{-1} d^{-1})**	**Carotenoids (mg L^{-1} d^{-1})**
0.2d^{-1}	0.70 ± 0.00 a	37.4 ± 2.1 a	0.15 ± 0.03 a
0.4d^{-1}	0.92 ± 0.06 b	73.5 ± 7.2 b	0.69 ± 0.19 b
0.6d^{-1}	0.55 ± 0.01 c	31.7 ± 2.1 a	0.41 ± 0.24 ab
	Stress phase		
	Biomass (g L^{-1} d^{-1})	**Lipids (mg L^{-1} d^{-1})**	**Carotenoids (mg L^{-1} d^{-1})**
0.2d^{-1}	0.43 ± 0.01 a	69.9 ± 4.7 a	1.04 ± 0.15 a
0.4d^{-1}	0.53 ± 0.02 b	89.0 ± 16.1 b	1.26 ± 0.17 a
0.6d^{-1}	0.35 ± 0.03 c	31.7 ± 3.5 c	0.33 ± 0.13 b

Table 3. Photosynthetic performance and optical properties of *Golenkinia* FAUBA-3 under semicontinuous cultures at steady-state condition and salinity stress. E_{av} = daily mean average irradiance inside the culture; Ka = biomass extinction coefficient; a* = *in vivo* chlorophyll absorption cross section; α * = initial slope of ETR* vs. PAR; $ETR^{*}max$ = maximum electron transport rate by chlorophyll unit; $ETR_{B}max$ = maximum electron transport rate by biomass unit; $E_{k\ PSII}$ = onset of irradiance saturating photosynthesis; $E_{opt\ PSII}$ = irradiance of the initial photoinhibition; NPQ*max* = maximum non-photochemical quenching. Data are the means and standard deviation of three replicate experiments. Different letters indicate significant differences of means ($p<0.05$).

	Semincontinuous cultures		
	0.2 d^{-1}	**0.4 d^{-1}**	**0.6 d^{-1}**
E*av* (μmol photons m^{-2} s^{-1})	56.5 ± 5.6 a	83.1 ± 4.9 a	260.3 ± 99.9 b
Ka (m^2 g DW^{-1})	0.13 ± 0.01 a	0.15 ± 0.02 a	0.13 ± 0.06 a
a* (m^2 mg Chl^{-1})	0.085 ± 0.006 a	0.018 ± 0.002 b	0.041 ± 0.002 c
α *	0.026 ± 3.E-04 a	0.005 ± 1.E-04 b	0.011 ± 5.E-04 c
ETRmax***	4.30 ± 0.40 a	1.09 ± 0.19 b	2.32 ± 0.13 c

(µmol e^- mg $Chla^{-1}$ s^{-1})												
$ETR_{B}max$ (µmol e^- g DW^{-1} s^{-1})	6.55	±	1.04	a	8.67	±	1.43	a	7.70	±	3.83	a
$E_{k\ PSII}$ (µmol photons m^{-2} s^{-1})	166.7	±	16.6	a	205.5	±	38.2	a	212.2	±	18.1	a
$E_{opt\ PSII}$ (µmol photons m^{-2} s^{-1})	1204.5	±	76.8	a	2141.0	±	610.0	b	1108.2	±	91.2	a
NPQ*max*	0.91	±	0.12	a	0.78	±	0.01	a	0.74	±	0.02	a

	Stress phase											
	0.2 d^{-1}				**0.4 d^{-1}**				**0.6 d^{-1}**			
E*av* (µmol photons m^{-2} s^{-1})	149.4	±	31.1	a	252.7	±	7.7	a	413.5	±	48.8	b
Ka (m^2 g DW^{-1})	0.08	±	0.02	a	0.07	±	0.00	a	0.07	±	0.01	a
a* (m^2 mg Chl^{-1})	0.032	±	0.008	ab	0.027	±	0.002	a	0.044	±	0.005	ab
α *	0.002	±	2.E-03	a	0.002	±	6.E-04	a	0.001	±	1.E-04	a

ETR*$_{max}$ (µmol e^- mg $Chla^{-1}$ s^{-1})	0.29	±	0.13	a	0.61	±	0.20	a	0.25	±	0.05	a
$ETR_B$$_{max}$ (µmol e^- g DW^{-1} s^{-1})	1.02	±	0.47	a	0.96	±	0.06	a	0.47	±	0.03	a
E_k PSII (µmol photons m^{-2} s^{-1})	116.0	±	49.2	a	433.4	±	240.4	ab	332.3	±	32.0	b
E_{opt} PSII (µmol photons m^{-2} s^{-1})	----	±	----	a	----	±	----	b	738.7	±	65.5	a
NPQ$_{max}$	0.39	±	0.09	a	0.29	±	0.03	ab	0.12	±	0.03	b

Table 4. Fatty acid profiles of Golenkinia FAUBA- 3 under semicontinuous cultures at steady-state condition and salinity stress at different dilution rates detected by GC-FID. Values are given as percentages of total FAMEs. Data are the means and standard deviation of three replicate experiments. Different letters indicate significant differences of means ($p<0.05$). SFAs = Saturated Fatty Acids; MUFAs = Monounsaturated Fatty Acids; PUFAs = Polyunsaturated Fatty Acids. The main fatty acids are highlighted in gray.

	Semicontinuos			Stress		
	0.2 day^{-1}	0.4 day^{-1}	0.6 day^{-1}	0.2 d^{-1}	0.4 day^{-1}	0.6 day^{-1}
C14:0	0.2 ± 0.0	0.2 ± 0.0	0.3 ± 0.0	0.4 ± 0.0	0.3 ± 0.2	0.3 ± 0.0
C14:1	0.5 ± 0.1	0.3 ± 0.4	1.0 ± 0.2	0.1 ± 0.0	0.0 ± 0.0	0.2 ± 0.1
C16:0	25.1 ± 1.1	23.4 ± 1.6	27.0 ± 0.9	21.2 ± 0.1	26.2 ± 6.4	25.9 ± 3.7
C16:1	0.4 ± 0.1	0.6 ± 0.0	1.4 ± 0.4	0.1 ± 0.0	0.1 ± 0.1	0.3 ± 0.1
C17:0	7.8 ± 0.8	9.4 ± 0.2	4.8 ± 0.5	8.0 ± 0.1	8.2 ± 2.4	5.4 ± 0.9
C18:0	3.6 ± 1.6	5.0 ± 0.5	6.5 ± 0.7	3.7 ± 0.0	3.0 ± 1.2	3.8 ± 0.3
C18:1n9c	12.1 ± 0.8	6.8 ± 0.0	6.5 ± 0.3	35.3 ± 0.8	29.7 ± 8.9	33.4 ± 2.4
C18:2n6c	33.4 ± 1.2	35.5 ± 0.2	26.3 ± 0.5	23.0 ± 0.5	22.3 ± 1.1	19.3 ± 1.4
C18:3n6	0.2 ± 0.0	0.1 ± 0.0	0.1 ± 0.0	0.2 ± 0.0	0.1 ± 0.1	0.4 ± 0.1
C18:3n3	13.3 ± 0.4	16.3 ± 1.1	23.9 ± 0.6	5.2 ± 0.1	8.2 ± 2.4	7.7 ± 0.3
C20:0	0.7 ± 0.0	0.4 ± 0.0	0.3 ± 0.0	0.9 ± 0.1	0.5 ± 0.5	0.7 ± 0.0
C20:1	0.3 ± 0.0	0.2 ± 0.0	0.2 ± 0.0	0.6 ± 0.0	0.5 ± 0.5	0.9 ± 0.0
C22:0	0.8 ± 0.0	0.4 ± 0.0	0.4 ± 0.1	0.6 ± 0.1	0.4 ± 0.3	0.5 ± 0.1
C22:1n9	0.6 ± 0.2	0.8 ± 0.0	0.6 ± 0.3	0.2 ± 0.0	0.1 ± 0.1	0.7 ± 0.5
C24:0	0.2 ± 0.0	0.1 ± 0.0	0.1 ± 0.0	0.2 ± 0.0	0.1 ± 0.1	0.1 ± 0.0

SFAs	38.7	±	1.1	a	39.1	±	1.4	a	39.6	±	1.1	a	35.1	±	0.2	a	38.8	±	6.3	a	36.9	±	3.2	a
MUFAs	14.0	±	0.6	a	8.7	±	0.4	b	9.7	±	0.6	b	36.4	±	0.8	b	30.5	±	9.7	b	35.6	±	1.7	b
PUFAs	47.3	±	1.1	a	52.2	±	1.0	b	50.7	±	0.9	ab	28.4	±	0.6	c	30.7	±	3.4	c	27.5	±	1.6	c

Supplementary Material

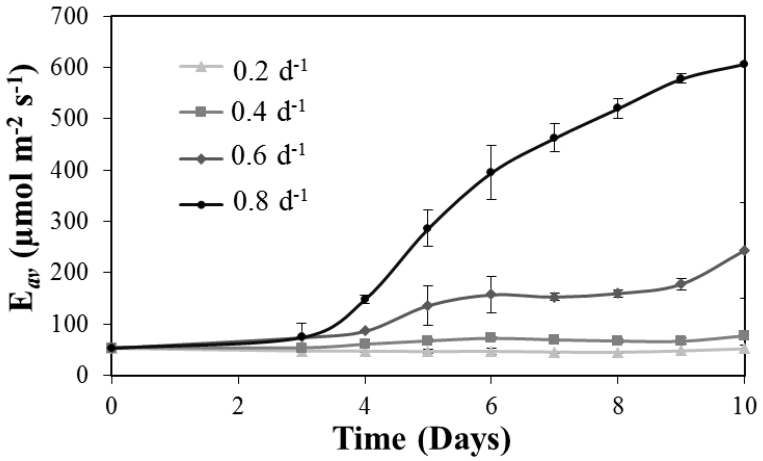

Figure S1. Time course of daily mean average irradiance inside the culture (E_{av}) at different dilution rates in semicontinuous cultres of *Golenkinia* FAUBA-3.

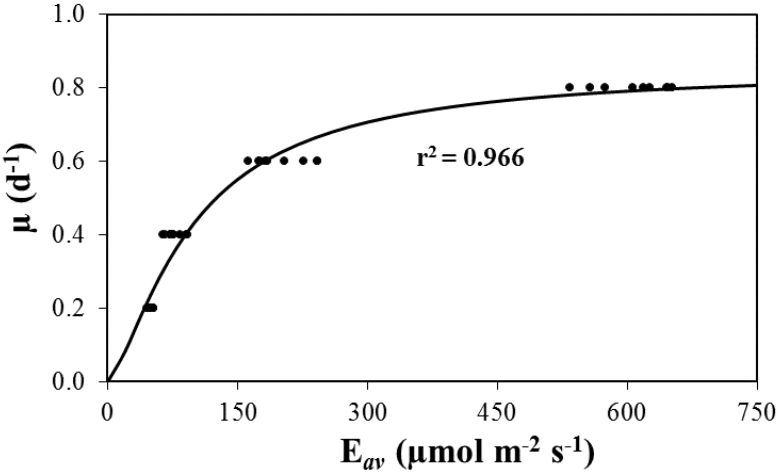

Figure S2. Variation of specific growth rate with the daily mean E_{av} of *Golenkinia* FAUBA-3. Points correspond to experimental data at steady state and the line corresponds to the model (Eq. 4) fitted by nonlinear regression.

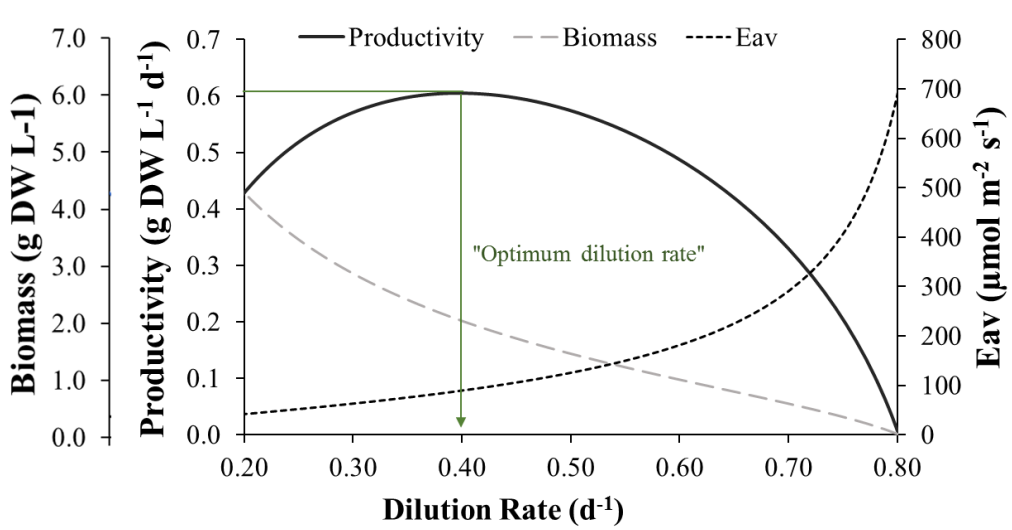

Figure S2. Simulation biomass concentration, biomass productivity and daily mean average irradiance inside the culture (Eav) at steady-state condition the model μ vs Eav (Eq. 4).